2
Basis of Chemical Reactor Design and Engineering

This chapter presents the fundamentals of chemical reaction engineering. It includes the basis of mass and energy balances, kinetics of homogenous reactions, including homogenous catalytic reactions in mono- and biphasic systems and kinetics of heterogenous catalytic reactions with special attention to the mass and heat transfer effects. Finally, the main design equations and comparative performance of three types of ideal reactors (Batch, Plug Flow, and Continuously Stirred Tank) are shortly summarized and discussed.

2.1
Mass and Energy Balance

The interactions between the chemical reaction and the simultaneously occurring transport processes for mass, energy, and impulse can be described by the fundamental conservation laws. At first the system boundaries must be specified. The volume enclosed by these boundaries is called *system volume*. The size of the system volume can be defined by natural boundaries, such as those of the phase boundary, the reactor, or by a small volume element of a phase through the defined limits of which mass, energy, and impulses can be exchanged (see Figure 2.1). For an unambiguous description, however, it is necessary to select the system volume in such a way that the conditions in it can be considered as uniform (e.g., constant temperature and concentrations).

The design of any chemical reactor is based on material and energy balance. A material balance has to be set for all species participating in the reactions taking place within the selected system volume. The material balance for a component A_i can be formulated in the following manner:

$$\left\{\begin{array}{c}\text{accumulation}\\ \text{of } A_i \text{ in}\\ \text{the system}\end{array}\right\} = \left\{\begin{array}{c}\text{rate of flow}\\ \text{of } A_i \text{ into}\\ \text{the system}\end{array}\right\} - \left\{\begin{array}{c}\text{rate of flow}\\ \text{of } A_i \text{ out of}\\ \text{the system}\end{array}\right\} + \left\{\begin{array}{c}\text{rate of production or}\\ \text{disappearance of } A_i\\ \text{into the system}\end{array}\right\}$$

$$\frac{\mathrm{d}n_i}{\mathrm{d}t} = \dot{n}_{i,0} - \dot{n}_i + P_i \qquad (2.1)$$

Microstructured Devices for Chemical Processing, First Edition.
Madhvanand N. Kashid, Albert Renken and Lioubov Kiwi-Minsker.

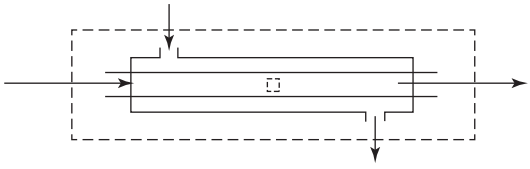

Figure 2.1 System volumes with differing selected sizes.

where n_i represents the number of moles of species A_i in the system at time t, $\dot{n}_i$ is the molar flow rate, and P_i is the rate of A_i production or disappearance. The last term in the above equation is often referred to as *source term*. The rate of A_i production/disappearance corresponds to the product of the system volume, ΔV, and the transformation rate R_i of the component A_i(Equation 2.2). The size of the system volume is chosen in such a way that inside the volume, concentrations and temperatures are constant.

$$P_i = R_i \cdot \Delta V \tag{2.2}$$

The rate of A_i transformation (R_i) is the sum of the rates (r_j) of the reactions in which A_i participates:

$$R_i = \sum_j \nu_{i,j} \cdot r_j \tag{2.3}$$

Much of this book deals with the finding of the expression that relates the P_i with different contacting patterns and various reaction parameters (intrinsic kinetic, reaction enthalpy, adiabatic temperature, etc.).

Concerning the classification of chemical reactions, different principles can be applied. One of the most useful for the reactor design is the classification based on the amount and types of the phases involved, such as homogenous reactions (takes place only in one phase) and heterogenous *reactions* (involves two or more phases). Treating the kinetics of homogenous reactions in order to optimize the performance of an eventual reactor is easier than treating heterogenous reactions. If for homogenous reactions the temperature, pressure, and composition are the main variables affecting the rate of transformations, for the heterogenous reactions the situation becomes more complex. The reaction can take place within one or multiple phases, at the interface, and reactants and products may be distributed between different phases. This implies that material has to move from phase to phase influencing the overall rate of transformation. In addition, the heat transfer may also play an important role and for highly exothermic/endothermic reactions may limit the overall transformation rates. The mass and heat transfers become increasingly important with the increase in temperature where the intrinsic reaction rates are very high.

The kinetics of homogenous and heterogenous reactions is discussed later in this chapter with a special attention on mass and heat transfer influence on the kinetics of heterogenous reactions.

Applying the principle of conservation of energy leads to the energy balance that can be described as follows:

$$\left\{\begin{array}{c}\text{rate of energy}\\ \text{accumulation}\\ \text{within}\\ \text{the system}\end{array}\right\} = \left\{\begin{array}{c}\text{rate of flow}\\ \text{of heat}\\ \text{to the system}\\ \text{from the}\\ \text{surroundings}\end{array}\right\} - \left\{\begin{array}{c}\text{rate of work}\\ \text{done by}\\ \text{the system}\\ \text{on the}\\ \text{surroundings}\end{array}\right\} + \left\{\begin{array}{c}\text{rate of energy}\\ \text{added to}\\ \text{the system}\\ \text{by mass flow}\\ \text{into the system}\end{array}\right\} - \left\{\begin{array}{c}\text{rate of energy}\\ \text{leaving the}\\ \text{system}\\ \text{by mass flow}\\ \text{out of the system}\end{array}\right\}$$

$$\frac{\mathrm{d}E_{\mathrm{sys}}}{\mathrm{d}t} = \dot{Q} - \dot{W} + \dot{E}_{\mathrm{in}} - \dot{E}_{\mathrm{out}} \tag{2.4}$$

The work term $\dot{W}$ is generally separated into flow work, $\dot{W}_f$, and shaft work, $\dot{W}_s$. Shaft work is, for example, from the stirrer in a stirred tank or a turbine in a tubular reactor. When the shear stress can be neglected, the work term is

$$\dot{W} = -\sum_i \dot{n}_i p \hat{V}_i|_{\mathrm{in}} + \sum_i \dot{n}_i p \hat{V}_i|_{\mathrm{out}} + \dot{W}_s \tag{2.5}$$

with $\hat{V}_i$, the molar volume of the reactant A_i.

Introducing these in Equation 2.4 results in

$$\frac{\mathrm{d}E_{\mathrm{sys}}}{\mathrm{d}t} = \dot{Q} - \dot{W}_s - \sum_i (\dot{E}_i + \dot{n}_i p \hat{V}_i)|_{\mathrm{in}} + \sum_i (\dot{E}_i + \dot{n}_i p \hat{V}_i)|_{\mathrm{out}} \tag{2.6}$$

The energy E_i is the sum of the internal energy, the kinetic energy, the potential energy, and all other energies such as electric, magnetic, or light. For the description of the majority of chemical reactors, the kinetic, potential, and other energies can be neglected, resulting in

$$\dot{E}_i \cong \dot{n}_i \hat{U}_i \tag{2.7}$$

Introducing the enthalpy

$$\hat{H}_i = \hat{U}_i + p\hat{V}_i \tag{2.8}$$

we obtain finally:

$$\frac{\mathrm{d}E_{\mathrm{sys}}}{\mathrm{d}t} = \dot{Q} - \dot{W}_s - \sum_i \dot{n}_{i,0} \hat{H}_{i,0} + \sum_i \dot{n}_i \hat{H}_i \tag{2.9}$$

The subscript "0" indicates inlet conditions while $\hat{H}_i$ and $\hat{U}_i$ are the molar enthalpy and molar energy, respectively.

2.2
Formal Kinetics of Homogenous Reactions

Kinetics is a key discipline for chemical reaction engineering. It relates the rate at which a chemical transformation occurs to macroscopic process parameters, like pressure, concentrations, temperature. Moreover, it enables to find a link between the observed transformation rates to a *reaction mechanism* that describes intimate interactions between individual molecules. For solving chemical reaction engineering problems we are mostly interested in practical situations, where relatively large quantities of matter are transformed.

In order to quantify the rate of a chemical transformation, we need to introduce some definitions. First, we distinguish between different types of reactions based on the form used to describe eventual chemical transformation, as *single* or *multiple* reactions. Usually this can be done from material balance after examining the stoichiometry between reacting materials and products. If a single stoichiometric equation can present the transformation, this is a *single reaction*. If more than one equation is necessary to present all observed components and their transformations, this it is a case of *multiple reactions*. The examples are as following:

Single irreversible reaction: $A_1 + A_2 \rightarrow A_3 + A_4$
Consecutive reactions (or reactions *in series*): $A_1 \rightarrow A_2 \rightarrow A_3$
Parallel reactions: $A_1 \rightarrow A_2$, $A_1 \rightarrow A_3$
Parallel-consecutive: $A_1 + A_2 \rightarrow A_3$, $A_3 + A_2 \rightarrow A_4$

More complicated schemes are also possible and present a combination of the listed reactions.

According to the International Union of Pure and Applied Chemistry (IUPAC) [1] the reaction rate in homogenous system is the change in the number of moles per unit of time and unit of volume because of the reaction divided by the stoichiometric coefficients. The reaction rate is always positive.

2.2.1 Formal Kinetics of Single Homogenous Reactions

Experimentally it was observed that the reaction rate depends on the concentrations of the reacting species and temperature. Very often a simple Power Rate Law (PRL) can be applied to describe this dependency. For the single irreversible reaction: $A_1 + A_2 \rightarrow$ products, the following equation results:

$$r = k \cdot c_1^{n_1} \cdot c_2^{n_2} \tag{2.10}$$

The exponents in Equation 2.10 are called the *reaction orders*. The reaction is n_1 order with respect to reactant A_1 and n_2 with respect to A_2. The overall reaction order is given by:

$$n = n_1 + n_2$$

The decomposition of N_2O_5 in the gas phase is the example of a formal first order reaction [2]:

$$N_2O_5 \rightarrow NO_2 + NO_3$$
$$A_1 \rightarrow A_2 + A_3$$
$$r = k_1 \cdot c_1 \tag{2.11}$$

An example for second order reactions is the formation of HI from hydrogen and iodine [2]

$$H_2 + I_2 \rightarrow 2HI$$
$$A_1 + A_2 \rightarrow 2A_3$$
$$r = k_2 c_1 c_2 \tag{2.12}$$

In general, formal kinetic equations are empirical, valid only within a limited domain of concentrations and temperatures.

The reaction rate constant (or coefficient) in Equation 2.10 is independent of the composition of the reaction mixture, but is strongly influenced by the temperature. In practically all cases, the rate constant can be described by the Arrhenius law:

$$k = k_0 \cdot \exp\left(\frac{-E_a}{RT}\right) \tag{2.13}$$

where k_0 is the preexponential or frequency factor, and E_a is the apparent activation energy of the reaction. This expression fits well with the experiments over a wide range of temperatures. The frequency factor is much less temperature-sensitive than the exponential term, and, therefore, its variation with temperature is masked allowing in the Arrhenius law to consider $k_0 = \text{const}$.

For most reactions, the activation energy lies in the range of 40–300 kJ mol^{-1}. Its value can be estimated (provided that E_a remains constant) from the reaction rates measured at constant concentrations but at two different temperatures using the Arrhenius law:

$$\ln\frac{k_2}{k_1} = \ln\frac{k\,(T_2)}{k\,(T_1)} = \frac{E_a}{R}\left(\frac{1}{T_1} - \frac{1}{T_2}\right) \tag{2.14}$$

The knowledge of E_a allows to predict the kinetic rate constant at different operation temperature (see example 2.1).

Example 2.1: Estimation of reaction rate constants at different temperatures.

What will be the increase of the rate constant for a temperature rise of 10 K? Calculate for the reaction with the activation energy of 100 kJ mol^{-1}, supposing a base temperature of (a) 25 °C and (b) 100 °C.

Solution:

$$k(T_2) = k(T_1)\exp\left(\frac{-E_a}{R}\left[\frac{1}{T_2} - \frac{1}{T_1}\right]\right)$$
$$\ln\frac{k(T_2)}{k(T_1)} = \frac{-E_a}{R}\left[\frac{1}{T_2} - \frac{1}{T_1}\right] = -\frac{1\cdot 10^5}{8.31}\left[\frac{1}{308} - \frac{1}{298}\right] = 1.31$$
$$\frac{k(T_2)}{k(T_1)} = 3.71 \quad \text{for a temperature increase from 25 to 35 °C}$$
$$\Rightarrow \frac{k(T_2)}{k(T_1)} = 2.32 \,\text{for a temperature increase from 100 to 110 °C}$$

2.2.2
Formal Kinetics of Multiple Homogenous Reactions

As it has already been mentioned, often more than one chemical equation is necessary to present all observed components and their transformations. In this case one talks about complex or *multiple reactions.* One of the simple examples of multiple reactions is a ***reversible reaction*** occurring in the reactor, which can be presented in the following way:

$$\begin{aligned} j = 1: \quad & \nu_{1,1}A_1 + \nu_{2,1}A_2 \rightleftharpoons \nu_{3,1}A_3 + \nu_{4,1}A_4 \\ j = 2: \quad & \nu_{3,2}A_3 + \nu_{4,2}A_4 \rightleftharpoons \nu_{1,2}A_1 + \nu_{2,2}A_2 \end{aligned} \tag{2.15}$$

The transformation rates (see Equation 2.3) for the species $A_1, A_{3;}$ are given by:

$$R_1 = \nu_{1,1}r_1 + \nu_{1,2}r_2; \quad R_3 = \nu_{3,1}r_1 + \nu_{3,2}r_2 \tag{2.16}$$

The reaction rates depend on the concentrations of the reacting species and can be described by a PRL:

$$r_j = k_j \cdot \prod_i c_i^{n_i} \tag{2.17}$$

where c_i is the concentration of reactant A_i and n_i is the reaction order with respect to A_i.

If $|\nu_i| = 1$ and both reactions are of first order for all the reactants A_i, Equation 2.16 can be rewritten:

$$R_1 = -1 \cdot k_1 c_1 c_2 + 1 \cdot k_2 c_3 c_4; \quad R_3 = +1 \cdot k_1 c_1 c_2 - 1 \cdot k_2 c_3 c_4 \tag{2.18}$$

A chemical reaction proceeds in the direction in which the free Gibbs energy, G, of the reaction mixture diminishes. When equilibrium is reached:

$$R_1 = R_3 = 0 \tag{2.19}$$

$$k_1 c_1^* c_2^* = k_2 c_3^* c_4^*; \quad K_c = \frac{k_1}{k_2} = \frac{c_3^* c_4^*}{c_1^* c_2^*} \tag{2.20}$$

If the thermodynamic activities of the reactants correspond to their concentrations, the equilibrium constant K_c can be estimated from the second law of thermodynamics:

$$K_c(T) \cong K(T) = \exp\left(\frac{-\Delta G^0}{RT}\right) \tag{2.21}$$

Taking the derivative of Equation 2.21, where

$$\Delta G^0 = \Delta H^0 - T\Delta S^0 \tag{2.22}$$

the ***van't Hoff equation*** can be obtained:

$$\frac{\mathrm{d}\ln K}{\mathrm{d}T} = \frac{\mathrm{d}}{\mathrm{d}T}\left(\frac{-\Delta G^0}{RT}\right) = \frac{\Delta H^0}{RT^2}$$

By integrating from the standard temperature (273 K) to the desired temperature T, we obtain the dependence of the equilibrium constant on the

reaction enthalpy (the superscript "0" indicates standard conditions: $T_{st} = 273\,\mathrm{K}$, $p_{st} = 10^5\,\mathrm{Pa}$):

$$\ln K = \ln K(273) + \int_{273}^{T} \frac{\Delta H^0}{RT^2}\mathrm{d}T \tag{2.23}$$

For gas phase reactions, the PRL can be expressed in partial pressures. If the ideal gas law can be applied, the reaction rate constants are related as follows:

$$k_{j,c} \cdot \prod_i c_i^{n_i} = k_{j,p} \cdot \prod_i p_i^{n_i}; \quad k_{j,p} \cdot (RT)^{n_i} = k_{j,c}$$
$$\text{with } p_i = \frac{n_i}{V} \cdot RT = c_i \cdot RT \tag{2.24}$$

where V is the volume occupied by the reaction mixture, n_i – is the total number of moles of A_i in the mixture, R is the gas constant, and T is the reactor temperature in Kelvin, c_i is the concentration of A_i in the reactor.

2.2.3 Reaction Mechanism

The reaction mechanism describes intimate interactions between individual molecules and represents a network of elementary reactions involved in an overall transformation. It is often much more complex than the stoichiometry of the reaction as its formal kinetics in the form of PRL suggests. An example is the gas phase reaction between NO_2 and CO described by the following stoichiometric equation:

$$NO_2 + CO \rightarrow NO + CO_2 \tag{2.25}$$

Experimentally, a second order with respect to NO_2 and a zero order with respect to CO is found:

$$r = k\, c_{NO_2}^2 c_{CO}^0 = k\, c_{NO_2}^2 \tag{2.26}$$

This PRL expression indicates that the reaction is not elementary meaning that it does not proceed via a collision between NO_2 and CO molecules. The mechanism has been studied and proposed to consist of two consecutives elementary steps [3]:

$$\begin{aligned} &NO_2 + NO_2 \rightarrow NO_3 + NO; \quad r_1 = k_1\, c_{NO_2}^2 \\ &\underline{NO_3 + CO \rightarrow NO_2 + CO_2}\ ; \quad r_2 = k_2\, c_{NO_3} c_{CO} \\ &NO_2 + CO \rightarrow NO + CO_2 \end{aligned} \tag{2.27}$$

The experimentally obtained formal kinetic equation (Equation 2.26) can be explained by a very fast second step compared to the first one ($r_2 \gg r_1$). In this case the overall transformation rate will be controlled by the rate of the first step as the slowest one being in agreement with the experimentally observed PRL equation. This method to derive a concentration term in the rate expression is called the "*rate-determining step*" approach.

Another useful and widely used approach is called the "*quasi steady-state approximation*" (QSSA). In this case we hypothesize the existence of at least one (or more) intermediates involved in the reaction mechanism whose concentration in the reacting mixture is very low and can be considered as quasi constant.

In general, formal kinetic models are valid only within a limited domain of concentrations and temperatures.

2.2.4 Homogenous Catalytic Reactions

The following types of homogenous catalytic reactions can be distinguished:

- Acid/base catalysis: substrate activation by protonation or deprotonation
- Nucleophilic/electrophilic catalysis: substrate activation by Lewis bases via electron pair donor complexes or by Lewis acids via electron pair acceptor complexes
- Organometallic complex catalysis: substrate activation via coordinative interaction [4]
- Enzyme catalysis: substrate activation by multifunctional interactions [5].

The kinetics of homogenous catalytic reactions are presented here for the acid/base and enzymatic catalysis as examples.

Acid/base catalysis is probably the oldest type of homogenous catalytic reactions. Following the definitions by Brønstedt [6] and Lowry [7], the acids are proton donators and the bases are proton acceptors. Let us consider a bimolecular catalytic reaction with the equation presented as following:

$$A_1 + A_2 \xrightarrow{HA} A_3 \tag{2.28}$$

The mechanism of this acid catalyzed reaction is depicted in Scheme 2.1

If the product formation is slow compared to the protonation reactions ($k_2 \ll k_1, k_{-1}$) the transformation depends only on the concentration of protons c_{H^+} and a fast preequilibrium can be considered.

$$r_2 = k_2 \cdot c_{X^+} \cdot c_2 \text{ the rate-determining step}$$

$$\text{with}: c_{X^+} = \frac{k_1}{k_{-1}} \frac{c_{H^+}}{K_a} c_1$$

$$r = k_2 \frac{k_1}{k_{-1}} \frac{1}{K_a} c_{H^+} \cdot c_1 \cdot c_2 = k' \cdot c_{H^+} \cdot c_1 \cdot c_2 \tag{2.29}$$

$HA + A_1 \underset{k_{-1}}{\overset{k_1}{\rightleftharpoons}} X^+ + A^-$: formation of activated substrate X^+ (protonation) (fast)

$X^+ + A_2 \xrightarrow{k_2} A_3 + H^+$: irreversible rection of the protonated substrate with A_2 (slow)

$H^+ + A^- \rightleftarrows HA$: equilibrium (fast)

Scheme 2.1 Acid catalyzed bimolecular reaction A_1, A_2: reactants; A_3: product; HA: acid as catalyst.

If the protonation of the substrate is rate determining ($k_2 \gg k_1$), the reaction rate is directly proportional to the concentration of the Brønstedt acid.

$$r = r_1 = k_1 \cdot c_{HA} \cdot c_1 \tag{2.30}$$

Examples for reactions of fast protonations (Equation 2.29) are ester hydrolysis and alcoholysis, inversion of sucrose, and the hydrolysis of acetals. The mutarotation of glucose and the dehydration of acetaldehyde hydrate are examples of slow protonations described with Equation 2.30.

In systems, homogenously catalyzed by organometallic complexes, the selectivity of the reaction can be controlled by the appropriate choice of ligands on the catalytic metallic center. Combining a catalytic active metal with ligands often allows the synthesis of organic compounds that are otherwise accessible only through complex multistep synthesis.

Kinetics of homogenously catalyzed reactions is mostly described with the Michaelis–Menten model [8]. The model was first published in the field of enzyme kinetics in the beginning of the twentieth century. According to this model, the catalyst reacts with the substrate, A_1 in a preequilibrium to form a catalyst substrate complex, $X^{\#}$, which reacts usually irreversibly to form the product, A_2.

Besides enzymatic reactions, many homogenously catalyzed hydrogenations follow Scheme 2.2. An example is the asymmetric hydrogenation dehydroamino acid derivatives with rhodium or ruthenium catalysts. On the basis of Scheme 2.2 the following rate equation can be derived:

$$\begin{aligned} r &= \frac{k_2 \cdot c_{\mathrm{cat},0} \cdot c_1}{K_M + c_1} \\ \text{with } K_M &= \frac{k_{-1} + k_2}{k_1} = \frac{c_{\mathrm{cat}} \cdot c_1}{c_{X^{\#}}}; \\ K_M &\cong \frac{k_{-1}}{k_1} \; if \; k_2 \ll k_{-1}; K_M \cong \frac{k_2}{k_1} \; if \; k_2 \gg k_{-1} \end{aligned} \tag{2.31}$$

For $k_2 \ll k_{-1,}$ the Michaelis constant K_M corresponds to the inverse stability constant of the catalyst substrate complex.

$$\mathrm{Cat} + A_1 \underset{k_{-1}}{\overset{k_1}{\rightleftharpoons}} X^{\#} \quad \text{equilibrium (fast)}$$

$$X^{\#} \xrightarrow{k_2} A_2 + \mathrm{Cat} \quad \text{the rate determining step (slow)}$$

$$C_{\mathrm{cat},0} + C_{\mathrm{cat}} + C_{X^{\#}}$$

Scheme 2.2 Reaction sequence and catalyst mass balance of the simple Michaelis–Menten model.

For $c_1 \gg K_M$, Equation 2.31 reverts to a zero order kinetics with regard to the reactant. For this situation the concentration of free catalyst is near zero and the reaction rate attains a maximum.

$$r_{\max} = k_2 \cdot c_{\text{cat},0}; c_{X^\#} \cong c_{\text{cat},0} \tag{2.32}$$

If, on the other hand, $c_1 \ll K_M$, the rate of the product formation depends on the concentration of the catalyst as well as the reactant A_1, both of the first order. This is illustrated in example 2.2.

$$r = k_2 \cdot c_{\text{cat},0} \cdot c_1 = r_{\max} \cdot c_1 \tag{2.33}$$

Example 2.2: Enzyme catalysis (Michaelis-Menten model).

The kinetics of glucose formation from lactose by means of ß-galactosidase was studied in a wide range of variables by Flaschel *et al.* [9]. The dependence of the reaction rate as the function of the lactose concentration is shown in Figure 2.2.

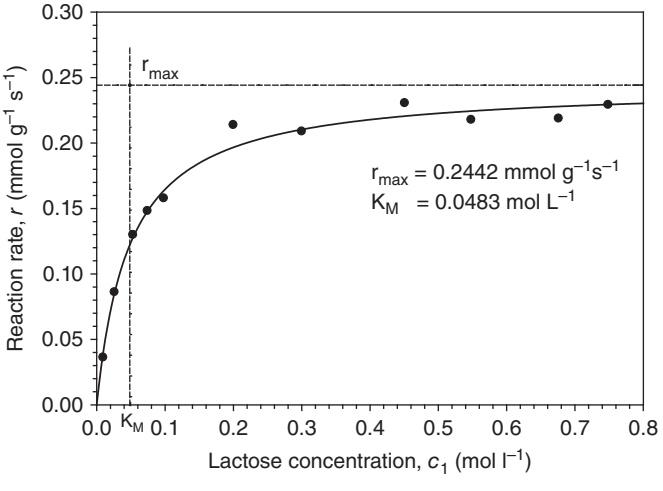

Figure 2.2 Initial rate of enzymatic lactose hydrolysis [10] ($T = 50\,°C$, pH = 3.5; $c_{\text{cat, 0}} = 0.125\ \text{g l}^{-1}$).

The experimental results fit well to the rate equation derived from a Michaelis–Menten model as seen in Figure 2.2. The two-model parameters are easily obtained by fitting the model (Equation 2.31) to the experiments. For $c_1 = K_M$, the reaction rate corresponds to half of the maximum value.

$$r_{c_1=K_M} = \frac{k_2 \cdot c_{\text{cat},0} \cdot c_1}{K_M + c_1} = \frac{k_2 \cdot c_{\text{cat},0} \cdot c_1}{c_1 + c_1} = \frac{1}{2} k_2 \cdot c_{\text{cat},0}$$

2.3 Ideal Reactors and Their Design Equations

Most chemical reactors used in practice can be classified according to some common criteria and assigned to the so-called basic or ideal reactor types. On the basis of the characteristics of ideal reactors, the complex interactions of chemical reaction kinetics, mass, heat, and impulse transport can be discussed in a general way. The behaviors of many actually used reactors approach the ideal types so that their fundamental relationships can be applied at least for a first reactor design. In other cases, the reactor behavior of real systems must be described with the help of models often containing the ideal reactors as individual elements (see Chapter 3).

For ideal reactors, highly simplified assumptions are used as the starting point, such as an ideal mixing down to the molecular level or a plug flow (piston type flow pattern). We distinguish between:

- the ideally mixed, batch-wise operated stirred tank reactor (BSTR),
- the ideally mixed, continuously operated stirred tank reactor (CSTR), and
- the ideal plug flow reactor (PFR).

2.3.1 Performance Parameters

Several terminologies are used in the chemical reaction engineering literature to represent the performance of both catalytic and noncatalytic chemical processes. The definitions that are commonly used are given as follows:

Conversion: It indicates the progress of the reaction and is defined as the ratio of the amount of the limiting reactant transformed and the total amount fed to the reactor. For the following parallel reactions

$$\begin{aligned} j = 1 &: \nu_{1,1}A_1 + \nu_{2,1}A_2 \rightarrow \nu_{3,1}A_3 + \nu_{4,1}A_4 \\ j = 2 &: \nu_{1,2}A_1 \rightarrow \nu_{4,2}A_4 \end{aligned} \tag{2.34}$$

the conversion of A_1 is given by

$$X_1 = X = \frac{n_{1,0} - n_1}{n_{1,0}} \tag{2.35}$$

where, $n_{1,0}$ and n_1 are the initial and final numbers of moles of A_1, respectively.

Yield: It is the amount of product formed in the reaction referred to the amount of the reactant fed to the reactor. Considering the reactions indicated in Equation 2.34 the yield of A_3 with respect to reactant A_1 is defined as:

$$Y_{3,1} = \frac{n_{3,0} - n_3}{n_{1,0}} \frac{\nu_{1,1}}{\nu_{3,1}} \tag{2.36}$$

The yield of A_3 referred to the reactant A_2 is defined as

$$Y_{3,2} = \frac{n_{3,0} - n_3}{n_{2,0}} \frac{\nu_{2,1}}{\nu_{3,1}} \tag{2.37}$$

Selectivity: The selectivity corresponds to the amount of the desired product formed with respect to the amount of the compound reacted:

$$S_{3,1} = \frac{n_{3,0} - n_3}{n_{1,0} - n_1} \frac{\nu_{1,1}}{\nu_{3,1}} \tag{2.38}$$

Thus, from Equations 2.35, 2.36, and 2.38 one can find that

$$Y_{3,1} = X_1 \cdot S_{3,1} \tag{2.39}$$

Instantaneous selectivity: As the reaction rates depend on the reactant concentrations, the instantaneous yield and selectivity can change with time or the location in the reactor. The instantaneous or differential selectivity is defined as the ratio between the rate of product formation and the rate of reactant transformation:

$$s_{3,1} = \frac{\nu_1}{\nu_3} \frac{R_3}{R_1} = \frac{\nu_1}{\nu_3} \frac{\mathrm{d}c_3}{\mathrm{d}c_1} \tag{2.40}$$

2.3.2 Batch Wise-Operated Stirred Tank Reactor (BSTR)

In a batch reactor, there is no inflow or outflow of reactants. It is a commonly used apparatus in the fine and pharmaceutical industry as well as in laboratories because of its flexibility and multifunctionality. The ideal stirred tank reactor is characterized by complete mixing down to the molecular level. Therefore, no concentration or temperature gradients exist. The system volume (Figure 2.1) corresponds to the volume occupied by the reaction mixture as indicated in Figure 2.3. As reactants are neither added nor removed during the reaction time (batch time), the mass balance Equation 2.1 simplifies to

$$\left\{ \begin{matrix} \text{rate of reactant} \\ \text{accumulation} \end{matrix} \right\} = \left\{ \begin{matrix} \text{rate of reactant} \\ \text{transformation} \end{matrix} \right\}$$

$$\frac{\mathrm{d}n_i}{\mathrm{d}t} = V \cdot R_\mathrm{i} = V \cdot \sum_\mathrm{j} \nu_\mathrm{ij} r_\mathrm{j} \tag{2.41}$$

The volume V occupied by the reaction mass may change, if the density of the reaction mixture varies during the reaction time as a result of the changing product composition and of physical processes like heating or cooling.

In contrast to mass, the BSTR can exchange heat through the reactor wall with the surroundings, resulting in a heat balance as:

$$(\overline{C}_w + m\bar{c}_p)\frac{\mathrm{d}T}{\mathrm{d}t} = U \cdot A \cdot (T_c - T) + V \sum_j r_j(-\Delta H_{r,j}). \tag{2.42}$$

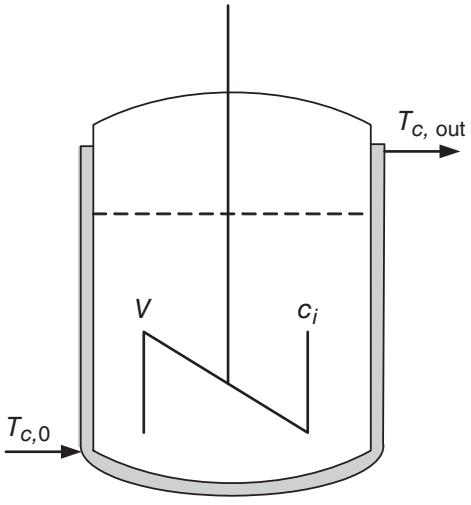

Figure 2.3 Batch-wise operated stirred tank reactor (BSTR).

with U the global heat transfer coefficient, A the heat exchange surface area of the reactor, T_c the mean temperature of the cooling/heating medium, and T the temperature of the reaction mixture.

The total heat capacity of the reactor is designated as $\overline{C}_w$ and is assumed to be independent of temperature. The same holds for the average specific heat $\bar{c}_p$ of the reaction mixture, for which it is additionally assumed that it does not change with the product composition. Equations 2.41 and 2.42 are used to describe the behavior of the reactor during the reaction period and to determine the reactor performance.

The reactor performance L_p is defined as the amount of product A_i produced per unit time. In batch-operated reactors, L_p depends on the entire reaction cycle t_{cycle}. The cycle consists of the reaction time t_R required to reach a desired degree of conversion and the shut-down time t_a needed for charging, emptying, cleaning, heating, and cooling of the reactor.

$$L_p = \frac{n_i - n_{i,0}}{t_a + t_R} = \frac{n_i - n_{i,0}}{t_{\text{cycle}}} \tag{2.43}$$

The term $n_{i,0}$ corresponds to the product present at the start of the cycle (usually $n_{i,\,0} = 0$).

The reaction time t_R, which is needed to achieve the desired degree of conversion, is obtained by integrating Equation 2.45. For a single reaction ($R_i = \nu_i \cdot r$) follows with X_f, the final degree of conversion of the key compound A_1:

$$X_f = \frac{n_{1,0} - n_{1,f}}{n_{1,0}} \tag{2.44}$$

$$t_R = n_{1,0} \int_{X_0}^{X_f} \frac{\mathrm{d}X}{(-R_1) \cdot V}. \tag{2.45}$$

The density of the reaction mixture may change during the transformation process. Examples are polymerizations, where often the density of the polymeric product is higher than the monomer. Density changes lead to a variation of the volume occupied by the reaction mixture, *V,* in the reactor.

If the reaction volume is a linear function of the conversion, we obtain the following relationship:

$$V = V_0 \cdot (1 + \alpha X) \tag{2.46}$$

The expansion factor α corresponds to the fractional volume change on complete conversion as defined in Equation 2.47.

$$\alpha = \frac{V_{X=1} - V_{X=0}}{V_{X=0}} \tag{2.47}$$

Introducing the expansion factor in Equation 2.45 we obtain:

$$t_R = n_{1,0} \int_0^{X_f} \frac{\mathrm{d}X}{(-R_1) \cdot V_0 \cdot (1 + \alpha X)} = c_{1,0} \int_0^{X_f} \frac{\mathrm{d}X}{(-R_1) \cdot (1 + \alpha X)} \tag{2.48}$$

For an irreversible *n*th order reaction with $-R_1 = k \cdot c_1^n = k \cdot c_{1,0}^n (1 - X)^n$, the reaction time is given by:

$$\begin{aligned} t_R &= \frac{1}{k \cdot c_{1,0}^{n-1}} \int_0^{X_f} \frac{(1 + \alpha X)^{n-1}}{(1 - X)^n} \mathrm{d}X, \\ \text{or } DaI &= \frac{t_R}{t_r} = t_R k c_{1,0}^{n-1} = \int_0^{X_f} \frac{(1 + \alpha X)^{n-1}}{(1 - X)^n} \mathrm{d}X \end{aligned} \tag{2.49}$$

DaI is the first Damköhler number, which is defined as the ratio of the residence time in the reactor (t_R) to the characteristic reaction time t_r as defined in Equation 2.50.

$$t_r = \frac{c_{1,0}}{(-R_{1,X=0})}; \quad t_r = \frac{1}{k \cdot c_{1,0}^{n-1}} \ (n\text{th-order reaction}) \tag{2.50}$$

For a first order reaction the necessary reaction time, respectively, the Damköhler number for a required conversion, is independent of the expansion factor and we obtain with

$$R_1 = -kc_1 = -kc_{1,0}(1 - X); \quad \frac{\mathrm{d}X}{\mathrm{d}t} = k(1 - X) \tag{2.51}$$

$$t_R = \frac{n_{1,0}}{V} \frac{1}{k \cdot c_{1,0}} \int_0^{X_f} \frac{\mathrm{d}X}{(1 - X)} = \frac{-1}{k} \ln(1 - X_f) \tag{2.52}$$

or

$$X_f = 1 - \exp(-k \cdot t_R) = 1 - \exp(-DaI) \tag{2.53}$$

The situation is different for reaction orders $n \neq 1$. For a second order reaction, integration of Equation 2.49 results in

$$DaI = t_R k c_{1,0} = \int_0^{X_f} \frac{(1 + \alpha X)}{(1 - X)^2} \mathrm{d}X = \frac{(1 + \alpha) X_f}{1 - X_f} + \alpha \ln(1 - X_f) \tag{2.54}$$

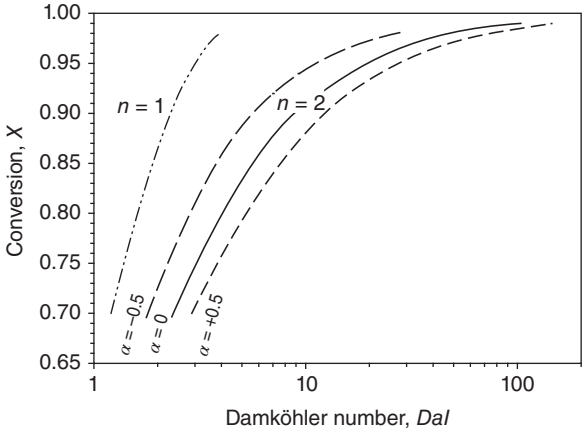

Figure 2.4 Conversion as function of the Damköhler number and the expansion factor.

In Figure 2.4 the influence of the expansion on the conversion in BSTR is illustrated for a second order reaction. The expansion has no influence on first order reactions in BSTR. Selectivity and yield obtained in BSTR are discussed in Examples 2.3 and 2.4 for parallel and consecutive reactions.

Example 2.3: Selectivity in BSTR for parallel reactions.

How the selectivity toward A_2 changes with the conversion of A_1 for parallel reactions and which value it will have if the rate constants are equal ($k_1 = k_2$)?

$$\nu_{11}A_1 \xrightarrow{k1} \nu_{21}A_2 \qquad \nu_{11} = \nu_{12} = -1; \quad \nu_{21} = \nu_{32} = +1$$
$$\nu_{12}A_1 \xrightarrow{k2} \nu_{32}A_3$$
$$n = 1$$

Solution:

$$S_{2,1} = \frac{k_1 c_1}{k_1 c_1 + k_2 c_1} = \frac{k_1}{k_1 + k_2}$$

The selectivity toward A_2, $S_{2,1}$ does not depend on the conversion and if the constants are equal, $S_{2,1} = 0.5$.

Example 2.4: Yield of the intermediate product as function of conversion.

Derive an expression and plot the concentration profiles for consecutive reactions (both of first order) with $k_2/k_1 = 0.5$. How the concentration and yield of A_2 changes with the conversion of A_1 and which value it will have if the

constants are equal?

$A_1 \xrightarrow{k_1} A_2 \xrightarrow{k_2} A_3$ Also propose an expression to estimate the yield of A_3.

Solution:

$$A_1 \xrightarrow{k1} A_2 \quad r_1 = k_1 c_1$$

$$A_2 \xrightarrow{k2} A_3 \quad r_2 = k_2 c_2$$

$$-\frac{\mathrm{d}c_1}{\mathrm{d}t} = k_1 c_1 \quad c_1 = c_{1,0}\exp(-k_1 t); \quad \Rightarrow X = 1 - f_1 = 1 - \frac{c_1}{c_{1,0}}$$

$$\frac{\mathrm{d}c_2}{\mathrm{d}t} = k_1 c_1 - k_2 c_2$$

$$c_2 = c_{1,0}\frac{k_1}{k_2 - k_1}[\exp(-k_1 t) - \exp(-k_2 t)]$$

$$Y_{2,1} = \frac{c_2}{c_{1,0}} = \frac{1}{\kappa - 1}[\exp(-DaI_1) - \exp(-\kappa \cdot DaI_1)] \text{ for } \kappa = \frac{k_2}{k_1} \neq 1$$

$$c_2 = k_1 t \cdot c_{1,0}\exp(-k_1 t)$$

$$Y_{2,1} = \frac{c_2}{c_{1,0}} = DaI_1 \cdot \exp(-DaI_1) \text{ for } \kappa = \frac{k_2}{k_1} = 1$$

The yield of the intermediate product passes through a maximum value as function of the time and the first Damköhler number, respectively. This is shown for first order consecutive reactions in Figure 2.5.

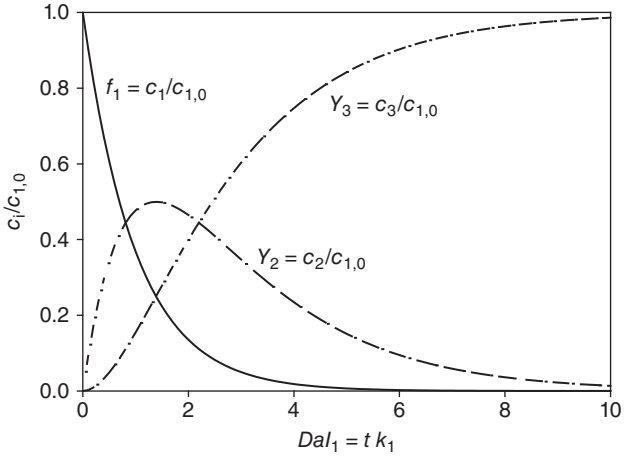

Figure 2.5 Product yields and unreacted fraction of the key reactant f_1 as function of the first Damköhler number. First order irreversible reaction, $\kappa = 0.5$.

The maximum yield of the intermediate depends only on the ratio of the rate constants $\kappa = k_2/k_1$ as shown in Figure 2.6. Decreasing κ results in an increasing maximum yield.

$$Y_{2,1,\max} = \frac{c_{2,\max}}{c_{1,0}} = \left(\frac{k_1}{k_2}\right)^{\frac{k_2}{k_2-k_1}} = \kappa^{\frac{\kappa}{1-\kappa}}; \text{for } \kappa \neq 1$$

$$Y_{2,1,\max} = \frac{c_{2,\max}}{c_{1,0}} = \frac{1}{\exp(\kappa)} \cong 0.368; \text{for } \kappa = 1$$

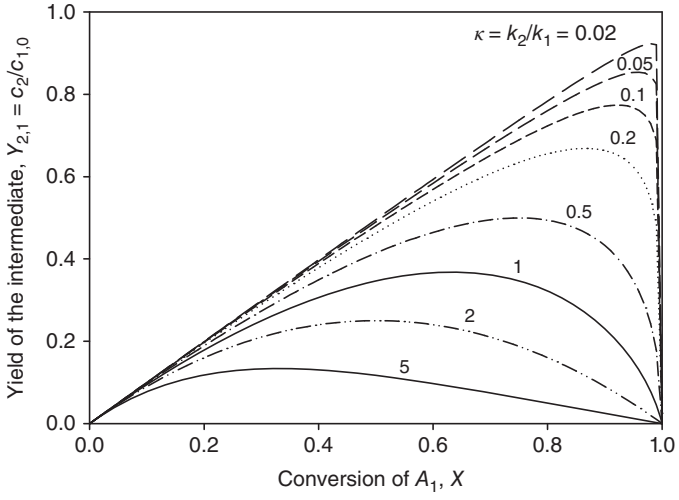

Figure 2.6 Yield of the intermediate product as function of the conversion and the ratio of rate constants. Irreversible first order reactions.

The yield of A_3 may be found from the mass balance:

$$c_1 + c_2 + c_3 = c_{1,0} \Rightarrow Y_{3,1} = 1 - f_1 - Y_{2,1}$$

2.3.3 Continuous Stirred Tank Reactor (CSTR)

One of the most important parameters to characterize continuous flow reactors is the degree of backmixing. In the ideal mixed reactor the concentrations and the temperature within the reactor volume are uniform. In consequence, the whole volume occupied by the reaction mixture can be taken as the system volume for the mass balance (see Figure 2.1).

In an ideal CSTR, the reactants fed to the reactor are instantaneously mixed up to the molecular level. The concentrations in the reactor correspond to the concentrations at the reactor outlet (Figure 2.7).

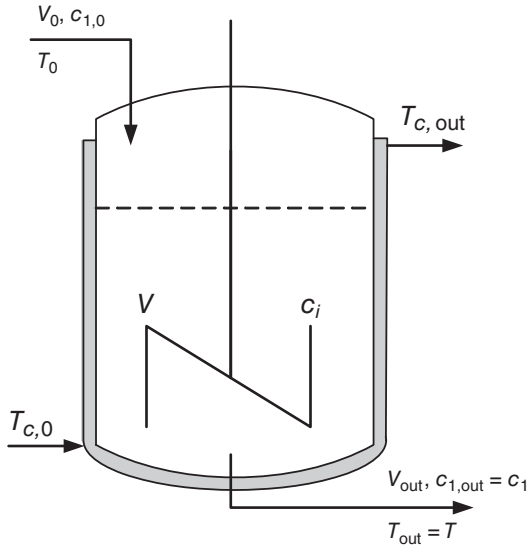

Figure 2.7 Continuous stirred tank reactor (CSTR).

When the molar flow $\dot{n}_i$ is replaced by the volumetric flow $\dot{V}$ and the concentration c_i, we obtain:

$$\frac{dn_i}{dt} = \dot{n}_{i,0} - \dot{n}_i + V \cdot R_i = V\frac{dc_i}{dt} = \dot{V}_0 c_{i,0} - \dot{V}_{out} c_{i,out} + V\sum_j \nu_{ij} r_j;\ (c_{i,out} = c_i) \tag{2.55}$$

The volume occupied by the reaction mixture is designated with *V*. In general, V corresponds to about three-fourth of the nominal reactor volume.

The ratio of the reaction volume to the volumetric inlet flow $\dot{V}_0$ is known as the *space time*:

$$\tau = \frac{V}{\dot{V}_0} \tag{2.56}$$

The reciprocal value of τ is often designated as the space velocity or, in biotechnology, the dilution rate.

After a transient period that corresponds to about five times the space time, the reactor operates at steady state, that is, the composition of the reaction mixture is time invariant and the mass balance is reduced to a simple algebraic expression.

$$\dot{V}_0 c_{i0} - \dot{V}_{out} c_{i,out} + V\sum_j \nu_{ij} r_j = \dot{V}_0 c_{i0} - \dot{V}_{out} c_{i,out} + V \cdot R_1 = 0 \tag{2.57}$$

Introduction of the degree of conversion for the key reactant A_1 leads to

$$X = \frac{\dot{n}_{1,0} - \dot{n}_{1,out}}{\dot{n}_{1,0}} = \frac{-V \cdot \sum_j \nu_{1,j} r_j}{\dot{V}_0 \cdot c_{1,0}} = \frac{V \cdot (-R_1)}{\dot{V}_0 \cdot c_{1,0}} \text{ or } \frac{V}{\dot{V}_0} = \frac{c_{1,0}}{\cdot(-R_1)} X \tag{2.58}$$

The space time necessary to achieve a required conversion is:

$$\tau = \frac{c_{1,0}X}{-R_1} \tag{2.59}$$

For reactions with *constant density* ($\rho_0 = \rho = \rho_{out}$) the volumetric inlet flow is identical to the volumetric flow at the outlet ($\dot{V}_0 = \dot{V}_{out}$) and the design equations for irreversible *n*th order reactions are readily found.

First order reaction		Second order reaction	
$A_1 \xrightarrow{k_1} A_2;\ r = k_1 \cdot c_1$		$A_1 \xrightarrow{k_1} A_2;\ r = k_2 \cdot c_1^2$	
$\dot{V}_0 \cdot (c_{1,0} - c_1) = V \cdot k_1 \cdot c_1$		$\dot{V}_0 \cdot (c_{1,0} - c_1) = V \cdot k_2 \cdot c_1^2$	
$1 - X = \frac{c_1}{c_{1,0}} = \frac{c_{1,out}}{c_{1,0}} = \frac{1}{1+k_1\tau}$		$1 - X = \frac{-1+\sqrt{1+4k_2c_{1,0}\tau}}{2k_2c_{1,0}\tau}$	
$1 - X = \frac{1}{1+DaI}$	(2.60)	$1 - X = \frac{-1+\sqrt{1+4DaI}}{2DaI}$	(2.61)

The necessary volume of the reaction mixture for a required performance (L_P, kmol s^{-1}) depends on the conversion of the key reactant A_1. This is summarized in Equations 2.62 and 2.63 for single reactions with a product selectivity of $S_{2,1} = 1 \Rightarrow L_P = \dot{n}_{2,out} = \dot{n}_{1,0}(1 - X) = \dot{V}_0 c_{1,0}(1 - X)$

$$V = \frac{L_P}{k_1 c_{1,0}(1 - X)} \tag{2.62}$$

$$V = \frac{L_P}{k_1 c_{1,0}^2 (1 - X)^2} \tag{2.63}$$

For reactions with **changing density** because of the transformation, the relations between conversion and space time depend also on the expansion factor α (Equation 2.47). For continuous flow reactors α is defined as follows:

$$\alpha = \frac{\dot{V}_{X=1} - \dot{V}_{X=0}}{\dot{V}_{X=0}} \tag{2.64}$$

The volume occupied by the reaction mixture depends on the arrangement of the outlet tubes and is, therefore, independent of the density. But, the outlet flow $\dot{V}_{out}$ is a function of the expansion factor.

$$\dot{V}_{out} = \dot{V}_0(1 + \alpha X) \tag{2.65}$$

In consequence, because of the density change, the mean residence time of the reaction mixture $\bar{t}$ is not identical to the space time ($\bar{t} \neq \tau$).

The design equations for CSTR with density change of the reaction mixture is based on the mass balance (Equation 2.57).

For single *n*th order reaction follows:

$$\dot{V}_0 c_{i0} - \dot{V}_{out} c_{i,out} + V \cdot R_1 = \dot{V}_0 c_{i0} - \dot{V}_{out} c_{i,out} + V \cdot (-k\, c_1^n) = 0 \tag{2.66}$$

The concentration of A_1 at the reactor outlet, which is identical with the concentration within the reactor, corresponds to the ratio between the molar outlet flow and the volumetric outlet flow.

$$c_1 = c_{1,\text{out}} = \frac{\dot{n}_{1,\text{out}}}{\dot{V}_{\text{out}}} = \frac{\dot{n}_{1,0} \cdot (1 - X)}{\dot{V}_0 \cdot (1 + \alpha X)} = c_{1,0} \frac{(1 - X)}{(1 + \alpha X)} \tag{2.67}$$

With the mass balance Equation 2.58, we can now determine the necessary space time, respectively, the necessary Damköhler number, for obtaining a required conversion.

$$\tau = \frac{V}{\dot{V}_0} = \frac{c_{1,0}}{-R_1} X = \frac{c_{1,0}(1 + \alpha X)^n}{k\, c_{1,0}^n (1 - X)^n} X$$

$$DaI = \tau\, k\, c_{1,0}^{n-1} = \frac{(1 + \alpha X)^n}{(1 - X)^n} X \tag{2.68}$$

It is important to emphasize the fact that even for first order reactions the density change influences the performance of continuously operated reactors in contrary to batch reactors. In Figure 2.8 the influence of the expansion factor on the conversion of first order reactions is demonstrated.

The heat balance at the steady state of the CSTR is expressed as:

$$\dot{V}_0 \rho_0 c_{p0} T_0 - \dot{V} \rho c_p T + U \cdot A(T_c - T) + V \sum_j r_j (-\Delta H_{r,j}) = 0. \tag{2.69}$$

For the simple case of a single reaction we obtain with the mass balance for the key component A_1

$$-R_1 V = r \cdot V = X c_{1,0} \dot{V}_0$$

$$\dot{V}_0 \rho_0 c_{p0} T_0 - \dot{V} \rho c_p T + U \cdot A(T_c - T) + \dot{V}_0 c_{1,0} X (-\Delta H_R) = 0 \tag{2.70}$$

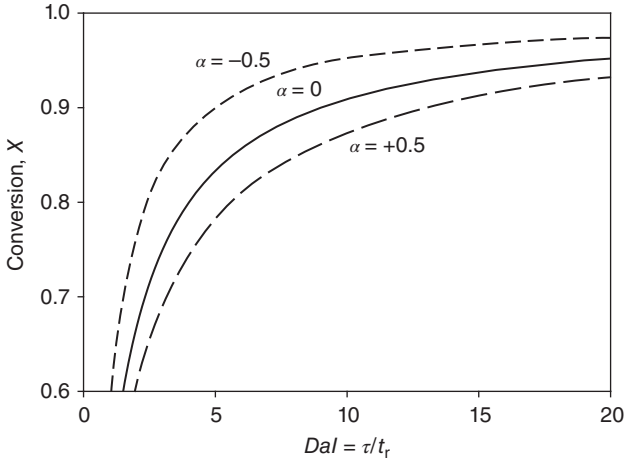

Figure 2.8 Conversion in a CSTR as function of the Damköhler number and the expansion factor for first order reactions.

or, at constant specific heat capacity ($c_p = c_{p,0}$)

$$\dot{V}_0 \rho_0 c_{p0}(T - T_0) + U \cdot A(T - T_c) = \dot{V}_0 c_{1,0} X(-\Delta H_R). \tag{2.71}$$

Together with the mass balance, Equation 2.71 serves for the design of the reactor, that is, to determine the operating parameters ($\dot{V}_0$, T_0, $c_{i,0}$) for a required reactor performance. It is important to note that CSTR, operating at steady state, can be operated isothermally. The cooling temperature T_c and the heat exchange area A can be adapted for known inlet temperatures T_0, and the required temperature inside the reactor, T (Figure 2.7).

2.3.4 Plug Flow or Ideal Tubular Reactor (PFR)

In contrast to the ideal CSTR, backmixing is excluded in an ideal tubular reactor, characterized by a plug flow pattern of the fluid, with uniform radial composition and temperature. The material balance for a small volume system element (ΔV) shown in Figure 2.9 at the reactor steady state is written as

$$-\frac{\mathrm{d}(c_i \dot{V})}{\mathrm{d}V} + \sum_j \nu_{ij} r_j = -\frac{\mathrm{d}(c_i u)}{\mathrm{d}z} + R_i = 0 \tag{2.72}$$

Any disturbance in the inlet flow travels with the linear velocity u through the reactor. Therefore, a novel stationary axial concentration profile is reached after the space time $\tau = V/\dot{V}_0$.

For a single, stoichiometrically independent reaction we obtain

$$\frac{\mathrm{d}\dot{n}_i}{\mathrm{d}V} = \frac{\mathrm{d}(c_i u)}{\mathrm{d}z} = \nu_i r = R_i. \tag{2.73}$$

After the introduction of the conversion for the key component A_1, the design equations for irreversible nth order reactions are readily found:

$$\frac{\mathrm{d}X}{\mathrm{d}V} = \frac{-R_1}{\dot{n}_{1,0}} = \frac{-R_1}{\dot{V}_0 \cdot c_{1,0}}. \tag{2.74}$$

The reactor volume required to achieve a target conversion can be calculated by integration.

$$V = \dot{n}_{1,0} \int_{X_0}^{X_L} \frac{\mathrm{d}X}{-R_1} \tag{2.75}$$

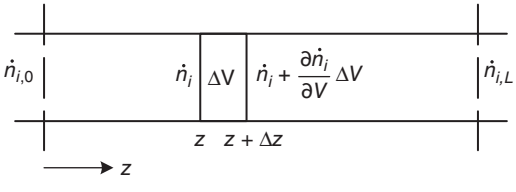

Figure 2.9 Ideal plug flow reactor.

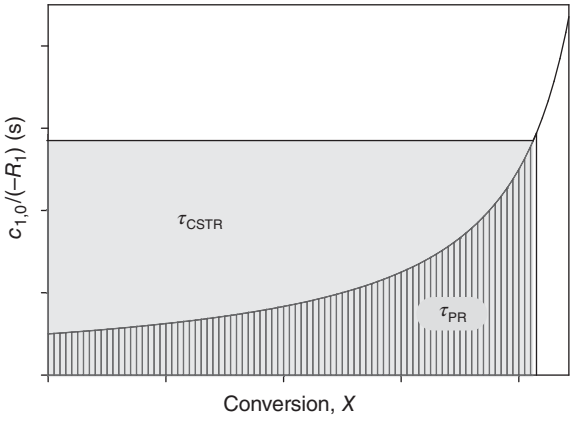

Figure 2.10 Space time in CSTR and PFR.

The space time in the reactor is then given by

$$\tau = \frac{V}{\dot{V}_0} = c_{1,0}\int_{X_0}^{X_L} \frac{\mathrm{d}X}{-R_1}. \tag{2.76}$$

The space time necessary for a required conversion corresponds to the hatched surface under the curve $c_{1,0}/(-R_1) = f(X)$ shown in Figure 2.10, which is for a reaction with positive order ($n > 0$). The space time in a CSTR is represented by the whole gray rectangle. Because of the low reactant concentration within a CSTR, the space time in the latter is considerably higher leading to a poor reactor performance.

For reactions with zero order ($n = 0$), the performance of CSTR and PFR are equal for any conversion. For the reactions with negative order, the transformation rate increases with decreasing reactant concentration and the performance of a CSTR will be higher compared to a PFR.

Reactions with *constant density* ($\rho_0 = \rho = \rho_{\text{out}}$):

If the density of the reaction mixture does not change throughout the reactor, the linear velocity of the reaction mixture remains constant and Equation 2.73 can then be transformed with $\mathrm{d}\tau = \mathrm{d}z/u$ to

$$u\frac{\mathrm{d}c_i}{\mathrm{d}z} = \frac{\mathrm{d}c_i}{\mathrm{d}\tau} = \sum_j \nu_{ij} r_j = R_i.; \quad \text{with } u = \frac{\dot{V}_0}{A_{cs}} = \text{constant}. \tag{2.77}$$

For single irreversible reactions we obtain:

$$\frac{\mathrm{d}c_1}{\mathrm{d}\tau} = R_1 = -k\,c_1^n;\ \tau = -\frac{1}{k}\int_{c_{1,0}}^{c_{1,L}} \frac{1}{c_1^n}\mathrm{d}c;\ \ DaI = \tau \cdot k\,c_{1,0}^{(n-1)} = \int_0^{X_L} \frac{1}{(1-X)^n}\mathrm{d}X \tag{2.78}$$

Integration leads to:

$$\tau k = DaI = -\ln\left(\frac{c_{1,L}}{c_{1,0}}\right) = -\ln(1-X_L) \qquad \text{for } n=1;\ \alpha=0$$

$$\tau k c_1^{n-1} = DaI = \frac{1}{n-1}\left[\left(\frac{c_{1,L}}{c_{1,0}}\right)^{1-n} - 1\right] = \frac{(1-X_L)^{1-n}-1}{n-1} \qquad \text{for } n\neq 1;\ \alpha=0 \quad (2.79)$$

The derived expressions for the ideal tubular reactor are the same as those for an ideal, batchwise operated stirred tank reactor. The reaction time t_R is replaced by the space time τ, that is, the conversion achieved in a batch reactor is identical to that in an ideal flow tube when the reaction time t_R and the space time τ are equal.

However, this comparison is no longer valid when the reaction is accompanied by a **density change,** which leads to variations in the linear velocity.

Because of the volume change of the reaction mixture, the reactant concentration changes not only by chemical transformation, but also by expansion. Supposing a linear dependency between reaction volume and conversion (Equation 2.64), the concentration of reactant A_1 at any point of the reactor is given by:

$$c_1 = \frac{\dot{n}_1}{\dot{V}} = \frac{\dot{n}_{1,0}\cdot(1-X)}{\dot{V}_0\cdot(1+\alpha X)} = c_{1,0}\frac{(1-X)}{(1+\alpha X)} \quad (2.80)$$

The concentration has to be introduced in the transformation rate expression and in the general design equation (Equation 2.76) for determining the space time for a required conversion. The space time can always be found by numerical or graphical integration. However, for simple kinetics analytical integration is possible. For the following *n*th order reactions analytical solutions are obtained:

General expression (Equation 2.76): $\tau = \frac{V}{\dot{V}_0} = c_{1,0}\int_{X_0}^{X_L}\frac{\mathrm{d}X}{-R_1}$.

Zero order reaction: $-R_1 = k;\ \ \tau = c_{1,0}\int_{X_0}^{X_L}\frac{\mathrm{d}X}{k}$.

$$DaI = \frac{k\tau}{c_{1,0}} = X \quad (2.81)$$

First order reaction: $A_1 \xrightarrow{k}$ products;

$$-R_1 = k c_1 = k c_{10}\frac{(1-X)}{(1+\alpha X)};\ \ \tau = k c_{1,0}\int_{X_0}^{X_L}\frac{(1+\alpha X)}{(1-X)}\mathrm{d}X$$

$$DaI = k\tau = -(1+\alpha)\ln(1-X) - \alpha X \quad (2.82)$$

Second order reaction: $2A_1 \xrightarrow{k}$ products;

$$-R_1 = k c_1^2 = k c_{1,0}^2\frac{(1-X)^2}{(1+\alpha X)^2};\ \ \tau = k c_{1,0}\int_{X_0}^{X_L}\frac{(1+\alpha X)^2}{(1-X)^2}\mathrm{d}X$$

$$DaI = k c_{1,0}\tau = 2\alpha(1+\alpha)\ln(1-X) + \alpha^2 X + (1+\alpha)^2\frac{X}{1-X} \quad (2.83)$$

The designs of reactors with volume change are illustrated in Example 2.5 and 2.6.

Example 2.5: Design of a plug-flow reactor for reactions with increasing volumetric flow.

According to K. M. Watson [11] the noncatalyzed dehydrogenation of butene to butadiene can be described by the following expressions:

$$C_4H_8 \rightarrow C_4H_6 + H_2$$

$$-R_1 = k \cdot p_1(\text{kmol} \cdot \text{h}^{-1} \cdot \text{m}^{-3})$$

$$k = 1.75 \cdot 10^{15} \exp\left(\frac{-30\,200}{T}\right) \text{kmol} \cdot \text{m}^{-3} \cdot \text{h}^{-1} \cdot 10^{-5}\,\text{Pa}^{-1}$$

Determine the space time in an isothermal plug flow reactor to achieve 90% conversion ($X = 0.9$) of butene under the following conditions:

$$T = 923\,\text{K}\ \dot{n}_{10} = 1\ \ \text{kmol} \cdot \text{h}^{-1}\ \ \text{butene}$$

$$p = 10^5\,\text{Pa}\ \dot{n}_1 = 1\ \ \text{kmol} \cdot \text{h}^{-1}\ \ \text{water vapor}$$

Solution:

The reaction is accompanied by a change in volume, as it is performed at constant pressure. The reaction mixture is assumed to behave as an ideal gas, so that the volume changes linearly with increasing butene conversion. As a mixture of butene and inert water vapor is employed, we obtain for the expansion factor:

$$\alpha = \frac{V_{X=1} - V_{X=0}}{V_{X=0}} = \frac{3-2}{2} = 0.5.$$

The partial pressure of butene is then given by

$$p_1 = \frac{\dot{n}_1 \cdot RT}{\dot{V}} = RT\frac{\dot{n}_{10}(1-X)}{\dot{V}_0(1+\alpha X)} = c_{10} \cdot RT\frac{1-X}{1+\alpha X}\ :$$

Substitution in the rate equation and the mass balance leads to

$$\tau = c_{10}\int_0^{X_L} \frac{\mathrm{d}X}{-R_1} = \frac{1}{k \cdot RT}\int_0^{X_L} \frac{(1+\alpha X)}{(1-X)}\mathrm{d}X$$

$$\tau = \frac{1}{k \cdot RT}[-\alpha X_L - (1+\alpha)\ln(1-X_L)].$$

Thus, after the insertion of the numerical values, we obtain:

$$\tau = \frac{10^5}{1.75 \cdot 10^{15}\exp(-30\,200/923) \cdot 8313\,\text{J} \cdot 923} \cdot 3.00 = 3.62 \cdot 10^{-3}\,\text{h} = 13\,\text{s}.$$

Example 2.6: Design equation for 1/2 order reaction with volume change.

The kinetics of a homogenous cracking reaction $A_1 \xrightarrow{k} 3A_2$ can be described with the following rate equation:

$$-R_1 = k\,c_1^{0.5};\ 450\,\mathrm{K} \le T \le 550\,\mathrm{K}; 4 \cdot 10^5\,\mathrm{Pa} \le p \le 6 \cdot 10^5\,\mathrm{Pa}$$

A PFR is operated at 500 K and $6 \cdot 10^5$ Pa with pure A_1 at the entrance. The initial concentration is $c_{1,0} = 0.528\,\mathrm{kmol\,m^{-3}}$ and the rate constant is found to be $k = 0.02\,\mathrm{kmol^{1/2}\,m^{-3/2}\,s^{-1}}$ under the reaction conditions.

Find the space time needed for a conversion of $X = 0.8$.

Solution:

For the given stoichiometry and with the pure reactant at the reactor entrance, one volume of the feed gas will give three volumes of product gas at full conversion. The expansion factor is $\alpha = (3-1)/1 = 2$.

Therefore, the transformation rate is given by:

$$-R_1 = k\,c_{1,0}^{1/2}\left(\frac{1-X}{1+2\cdot X}\right)^{1/2}$$

For the design equation (Equation 2.76) we obtain

$$\tau = c_{1,0}\int_0^{X_L} \frac{1}{k\,c_{1,0}^{1/2}}\left(\frac{1+2X}{1-X}\right)^{1/2}\mathrm{d}X$$

or, by introducing the Damköhler-number:

$$DaI = \tau k\,c_{1,0}^{-1/2} = \int_0^{X_L}\left(\frac{1+2X}{1-X}\right)^{1/2}\mathrm{d}X$$

The necessary Damköhler number for a required conversion can be obtained by plotting $\sqrt{(1+2X)/(1-X)}$ as function of X and determining the area under the curve between the initial and final conversion as shown in Figure 2.11a.

A simple way to estimate the area under the curve is to use the trapezoidal rule. In this case we break up the function into a number of trapezoids and calculate their areas. The area under the curve is then approximated by the sum of the trapezoids as shown in Figure 2.11b. The accuracy of the numerical integration increases with decreasing spaces between the points.

In the present example with four trapezoids, the area under the curve is estimated to be $DaI = \int_0^{0.8}\sqrt{(1+2X)/(1-X)}\,\mathrm{d}X \cong 1.54$.

The required space time for obtaining a conversion of $X = 0.8$ is:

$$\tau = DaI \cdot \frac{\sqrt{c_{1,0}}}{k} \cong 1.54 \cdot \frac{\sqrt{0.528}}{0.02} = 56\,\mathrm{s}$$

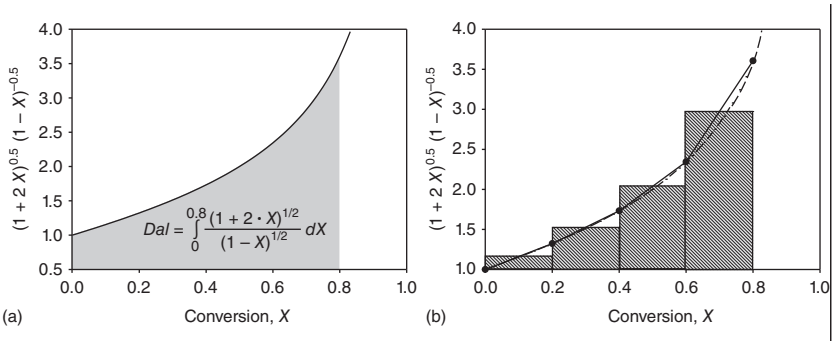

Figure 2.11 (a, b) Determining the Damköhler number for a given conversion.

The ***heat balance*** for a volume element in an ideal PFR at steady state can be formulated as follows:

$$\dot{m}\bar{c}_p \frac{\mathrm{d}T}{\mathrm{d}V} = \sum_j r_j(-\Delta H_{r,j}) + U(T_c - T)\frac{\mathrm{d}A}{\mathrm{d}V}. \tag{2.84}$$

In accord with the previously made assumptions, the temperature over the cross section is constant and only a function of the axial position. The term $(\mathrm{d}A/\mathrm{d}V)$ corresponds to the reactor surface per volume element (specific surface area, a). For circular tubes with a constant diameter d_t follows:

$$a = \frac{\mathrm{d}A}{\mathrm{d}V} = \frac{4}{d_t} \tag{2.85}$$

In general, the heat exchanged through the tube wall will be different from the heat generated or consumed by the reaction at the same axial position. As a consequence, an axial temperature profile develops. Exceptions are reactions with formally zero order, which doesn't depend on the reactant concentration.

To determine the axial temperature and concentration profiles, heat and mass balances must be solved simultaneously. For a single, stoichiometrically independent reaction and under stationary conditions, we obtain for the key component A_1

$$\frac{\mathrm{d}X}{\mathrm{d}Z} = \frac{-R_1 \cdot \tau}{c_{1,0}} \tag{2.86}$$

$$U\,a(T_c - T) + r(-\Delta H_r) - \dot{m}\bar{c}_p \frac{\mathrm{d}T}{\mathrm{d}V} = 0$$

$$\frac{\mathrm{d}T}{\mathrm{d}Z} = \frac{U \cdot \tau}{\rho_0 \cdot \bar{c}_p}\left(\frac{\mathrm{d}A}{\mathrm{d}V}\right)(T_c - T) + \Delta T_{\mathrm{ad}} \frac{r \cdot \tau}{c_{1,0}} \tag{2.87}$$

$Z = z/L$ (relative length of the reactor)

The heat management of tubular reactors is discussed in detail in Chapter 5.

2.4
Homogenous Catalytic Reactions in Biphasic Systems

A drawback of homogenous catalytic processes is often the complex and costly separation and recycling of the catalyst. Therefore, considerable efforts are made to combine the easy separation of heterogenous catalysts with the high potential activity and selectivity of homogenous molecular catalysts.

Different methods are proposed to facilitate the recovery of the catalyst. A very successful way is to use biphasic systems of two immiscible liquids. The catalyst should be soluble only in one phase, in which the transformation takes place, while the products and sometimes the reactants should be preferentially soluble in the second. The catalyst is thus "immobilized" within a "liquid support." The immiscible liquids can be separated after the reaction and the catalyst is recycled. This can be done without any thermal or chemical treatment. As the reaction is carried out in the presence of dissolved catalyst, the advantages of homogenous catalysis are fully preserved.

The liquid support may be water, supercritical fluids, ionic liquids, organic liquids or fluorous liquids [12]. The Shell higher olefin process (SHOP) and the Oxo synthesis (hydrofomylation) are examples of important industrial processes based on biphasic catalytic systems.

As the reaction takes place in the catalyst containing phase, the reactants must, first of all, be transferred from the second and eventually gas phase to the reaction phase. Therefore, special attention has to be paid to the mixing and dispersion of one phase within the other and mass transfer efficiency between phases. The mass transfer rate between the different phases depends on the area of the interface and the mass transfer coefficient. Whether the reaction will take place in the bulk of the reaction phase or near the interface depends on the ratio between the characteristic reaction time (t_r) and the characteristic time for mass transfer (t_m). This ratio is known as the *Hatta number* (*Ha*).

The discussion can be facilitated on the basis of the film model and by supposing a first order irreversible reaction in the reaction phase and neglecting the mass transfer resistance in the non-reactive phase I [13–15].

$$Ha = \sqrt{\frac{t_m}{t_r}} = \delta_{II}\sqrt{\frac{k'}{D_{1,II}}} = \frac{\sqrt{k' D_{1,II}}}{k_{L,II}} \tag{2.88}$$

With δ_{II}: the thickness of the boundary layer; k': the reaction rate constant, which is a function of the catalyst concentration ($k' = k \cdot c_{\text{cat}}$); $D_{1,II}$: the diffusion coefficient for the compound 1 in the second liquid phase; and k_L: the mass transfer coefficient in this liquid phase (phase II).

Depending on the value of *Ha,* different regimes can be distinguished (Figure 2.12): For $\boldsymbol{Ha \leq 0.3}$ the reaction rate is slow compared to the mass transfer and the reaction takes place in the bulk phase (Figure 2.12a). In this case, the mass transfer can be considered as an additional resistance in series to the

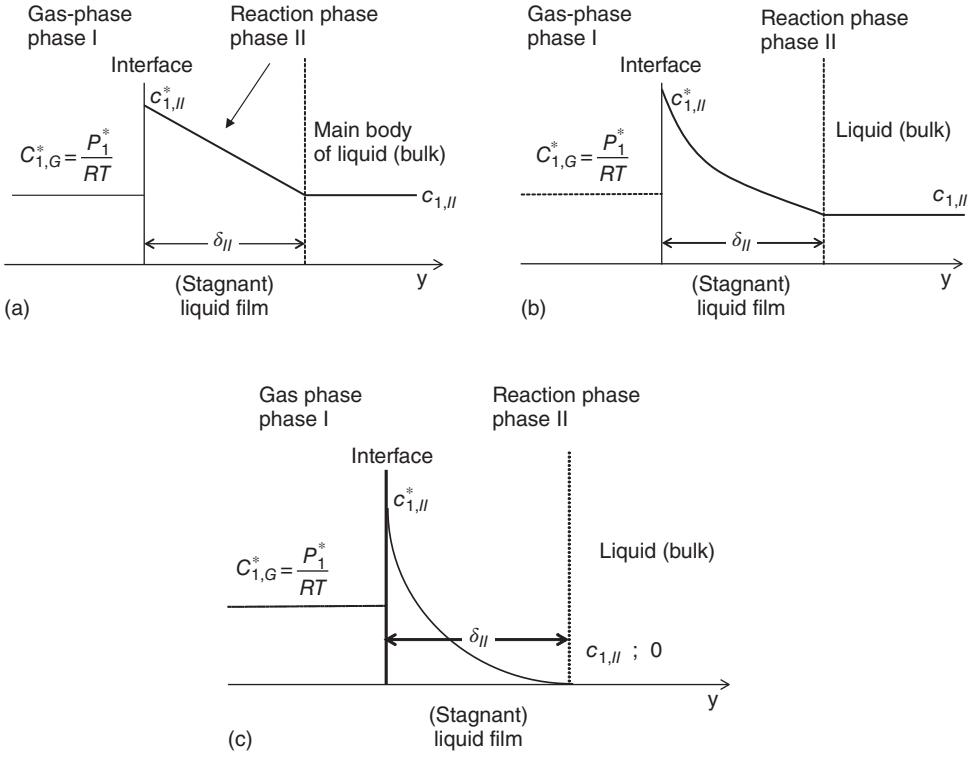

Figure 2.12 Concentration profiles for mass transfer with pseudo first order chemical reaction (film model) (a) slow chemical reaction: $Ha \leq 0.3$; (b) moderate chemical reaction: $0.3 \leq Ha \leq 3.0$; and (c) fast chemical reaction: $Ha \geq 3.0$. (Adapted from Ref. [15], Figure 4.20 Copyright © 2012, Wiley-VCH GmbH & Co. KGaA.)

reaction. The effective (observed) reaction rate is given by:

$$r_{ov} = \left(\frac{1}{k_L a} + \frac{1}{k'} \right)^{-1} c_{1,II} \tag{2.89}$$

For values of the Hatta number of $\mathbf{0.3 \leq Ha \leq 3,}$ the reaction takes place partially in the boundary layer and in the bulk of phase II. This leads to the deformation of the concentration profile in the stagnant film from the straight line as presented in Figure 2.12b. The overall rate of reaction is given by the reaction in the bulk at reactant concentration $c_{1,II}$ and in the boundary layer. This leads to the following expression for the observable effective rate:

$$r_{eff} = \frac{Ha}{\tanh Ha} \left[1 - \frac{c_{1,II}}{c^*_{1,II}} \cdot \frac{1}{\cosh Ha} \right] \cdot k_L a \cdot c^*_{1,II} \tag{2.90}$$

The bulk concentration $c_{1,II}$ is a rather complex function of the intrinsic reaction rate, the mass transfer coefficient, and the area of the interface [15].

$$\frac{c_{1,II}}{c^*_{1,II}} = \frac{1}{\cosh Ha[1 + Ha(1/B - 1) \cdot \tanh Ha]} \tag{2.91}$$

where $B = A \cdot \delta_{II}/V_{II} = V_{\text{film}}/V_{II}$ corresponds to the ratio between the film volume (V_{film}) and the volume of the reacting phase (V_{II}). Practical values for B are found to be in the range between $B = 0.1$ (for highly efficient fluid/fluid contactors) and $B = 2 \cdot 10^{-4}$. Therefore, for $Ha > 1$ the concentration in the bulk phase can be neglected ($c_{1,II}/c^*_{1,II} \cong 0$) and the effective rate becomes:

$$r_{\text{eff}} \cong \frac{Ha}{\tanh Ha} \cdot k_L a \cdot c^*_{1,II}, Ha > 1 \tag{2.92}$$

A further increase of the intrinsic reaction rate at constant volumetric mass transfer coefficient ($k_{\text{L,II}}$·a) results in Hatta numbers greater than 3 (***Ha* > 3**). The reaction rate can be considered as very fast compared to the mass transfer rate. As a consequence, the reactants do not reach the bulk phase ($c_{1,II} \approx 0$); the reaction takes place only in the boundary layer (Figure 2.12c). Under these conditions, the reaction rate increases proportionally with the specific interfacial area between the phases (a), the square root of the reaction rate constant, and the catalyst concentration as indicated in Equation 2.93.

$$r_{\text{eff}} = k_{L,II} \cdot a \cdot Ha \cdot c^*_{1,II} = \sqrt{k' \cdot D_{1,II}} \cdot a \cdot c^*_{1,II} = \sqrt{k \cdot c_{\text{cat}} \cdot D_{1,II}} \cdot a \cdot c^*_{1,II}, \; Ha \geq 3 \tag{2.93}$$

Example 2.7: Influence of catalyst concentration on the effective reaction rate.

Catalytic hydrogenation is carried out in a two-phase batch reactor, with the rate proportional to the catalyst concentration in the reaction phase.

The intrinsic reaction rate was found to be $k' = k \cdot c_{\text{cat}} = 1.12 \cdot 10^2\,\text{s}^{-1}$.

From the literature data it was found: $k_L = 5 \cdot 10^{-4}\,\text{m s}^{-1}$ $D_1 = 5 \cdot 10^{-9}\,\text{m}^2\,\text{s}^{-1}$

If one wants to double the effective hydrogenation rate, how should the concentration of the catalyst be changed?

Solution:

$$Ha = \frac{\sqrt{D_1 \cdot kc_{\text{cat}}}}{k_L} = 1.5 \; r_{\text{eff}} \cong \frac{Ha}{\tanh Ha} \cdot k_L a \cdot c^*_{1,II}, r_{\text{eff}} \cong \frac{1.5}{0.91} \cdot k_L a \cdot c^*_{1,II}$$

To double the hydrogenation rate, we obtain (From Equation 2.92 and 2.93):

$$r_{\text{eff},2} = 2 \cdot r_{\text{eff},1}; \quad \frac{r_{\text{eff},2}}{r_{\text{eff},1}} = \frac{Ha_2 \cdot k_L a \cdot c^*_{1,II}}{\frac{Ha_1}{\tanh Ha_1} \cdot k_L a \cdot c^*_{1,II}} = 2$$

$$Ha_2 = 2 \cdot \frac{Ha_1}{\tanh Ha_1} = 2 \cdot \frac{1.5}{0.91} = 3.3$$

$$\Rightarrow \frac{Ha_2}{Ha_1} = 2.2 = \sqrt{\frac{c_{\text{cat},2}}{c_{\text{cat},1}}} \Rightarrow c_{\text{cat},2} = 4.84 \cdot c_{\text{cat},1}$$

So, the catalyst concentration must be approximately fivefold higher in order to double the hydrogenation rate.

In summary, high *Ha* values lead to low reactant concentration in the reacting bulk phase and, as a consequence, the available volume of the reacting phase is less and less utilized. This situation can be characterized by introducing an efficiency factor η. The efficiency factor is defined as the ratio between the observed effective rate and the maximum production rate (controlled by the intrinsic kinetics) referred to the reactor volume (V_R) and corresponding to the maximum reactant concentration in the reacting phase ($c_{1,II} = c^*_{1,II}$):

$$\eta = \frac{r_{\text{eff}}}{r_{\max}}; r_{\max} = k' \frac{V_{II}}{V_R} c^*_{1,II} \tag{2.94}$$

The reactor efficiency depends on the *Ha*-number and the specific interfacial area. For a first order irreversible reaction the following relationship is obtained:

$$\eta = \frac{B}{Ha}\left[\frac{\tanh(Ha) + (B^{-1} - 1)Ha}{1 + (B^{-1} - 1)Ha \tanh(Ha)}\right] \text{ with } B = \frac{a \cdot V_R \cdot D_{1,II}}{V_{II} \cdot k_L} \tag{2.95}$$

The parameter B can be interpreted as the ratio between the film volume (V_{film}) and the volume of the reacting phase (V_{II}). In Figure 2.13 the efficiency factor as

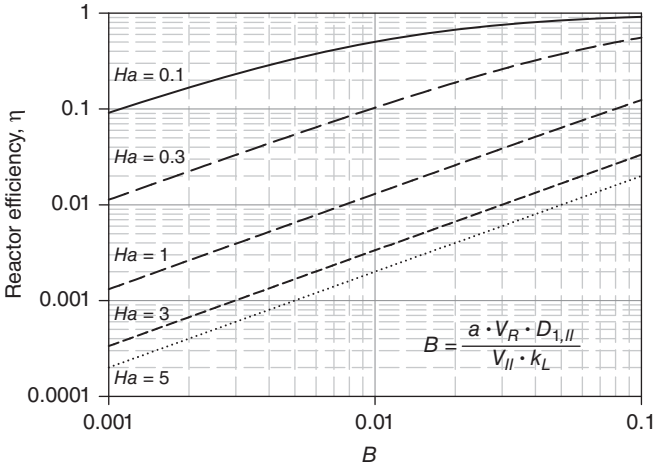

Figure 2.13 Effectiveness factor for fluid/fluid reactions as function of *Ha* and *B*. (Adapted from Ref. [16], Figure 4.21 Copyright © 2012, Wiley-VCH GmbH & Co. KGaA.)

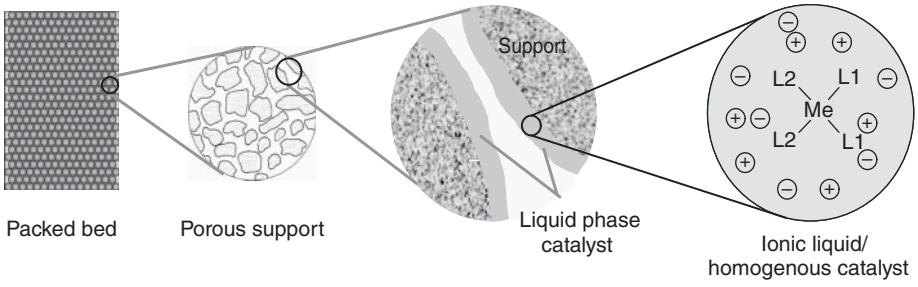

Figure 2.14 Schematic presentation of the concept of supported liquid phase catalysis. (Adapted from Ref. [16], Figure 4.22 Copyright © 2012, Wiley-VCH GmbH & Co. KGaA.)

function of *Ha* and *B* is shown. It clearly demonstrates that the reactor efficiency decreases with increasing *Ha* and with decreasing specific interfacial area *a.*

These relations are strictly valid only for simple irreversible first order reactions, but appropriate models for more complex kinetics can accordingly be developed based on the film model.

As shown above, fast chemical transformations characterized by $Ha \geq 3$ occur mainly near the interface and thus are limited by the interfacial area, which must be continuously generated by vigorous stirring of the multiphase mixture.

A possibility to overcome this drawback consists of immobilizing the liquid on a highly porous support. In this way a thin liquid layer is formed on the solid support leading to the desired high fluid/fluid interface. This approach is called *supported liquid phase catalyst* (SLPC) and combines the advantages of homogenous catalysis with a heterogenous fluid/solid system discussed in the following section. SLPC can be used like traditional heterogenous catalysts in packed bed reactors or even in fluidized beds. A schematic representation is shown in Figure 2.14.

The main problem related to SLPC is the loss of solvent because of evaporation in a continuously operated catalytic reactors. This problem can be overcome by using ionic liquids as solvent [17–20]. Ionic liquids are molten salts and their partial pressure is low under conditions commonly used for hydroformylation and hydrogenation reactions. As generally observed for SLPC, the catalytic activity and product selectivity depends on the liquid loading and the nature of the porous support [21]. A detailed discussion can be found in [22]. In order to diminish internal diffusion resistances within the supported liquids by using microstructured supports with high porosity like foams or fibrous materials, are proposed for SLPC [23].

2.5
Heterogenous Catalytic Reactions

The advantage of the heterogenous catalysis over homogenous is the easy postreaction separation of the catalyst which can further be used after regeneration and

the possibility to apply open reactors (flow processes). The chemical transformation occurs through new reaction pathways, which usually have lower energies of activation compared to the noncatalyzed reaction, and through formation of adsorption complexes.

In a few cases, the kinetics of heterogenous catalyzed reactions is based on a complete knowledge of the underlying reaction mechanisms. Generally, the kinetics of many commercially important reactions are derived from experimental investigations and are often based on simplified reaction models.

2.5.1 Rate Equations for Intrinsic Surface Reactions

No catalytic reaction can be elementary as at least three steps are always involved: adsorption of the reactant, surface reaction and desorption of the formed product. For a simple monomolecular reaction, for example, an isomerization, the steps involved are shown in Figure 2.15.

To describe the catalytic reaction, the catalyst must be included in the catalytic cycle as a participating species. The simplest way to do so is to consider a solid catalyst as an ensemble of single active sites (*). The transformation from A_1 to A_2 can be presented as a sequence of elementary steps:

$$\begin{aligned}
&A_1 + * \underset{k_{-1}}{\overset{k_1}{\rightleftharpoons}} A_1^* && \text{reactant adsorption/desorption}\\
&A_1^* \underset{k_{-2}}{\overset{k_2}{\rightleftharpoons}} A_2^* && \text{reversible surface reaction}\\
&A_2^* \underset{k_{-3}}{\overset{k_3}{\rightleftharpoons}} A_2 + * && \text{product desorption/adsorption}\\
&\overline{A_1 \rightleftharpoons A_2}
\end{aligned} \tag{2.96}$$

The adsorption of the reactant is herein considered as a reaction with an empty site (*) to give an adsorbed intermediate A_1^*. All sites are considered as equivalent and each can be occupied by a single species only.

Considering all steps as elementary reactions, expressions for the rate of each step can be obtained:

$$R_{ad} = r_1 - r_{-1} = k_1 p_1 Z_{tot} \theta_\nu - k_{-1} Z_{tot} \theta_1 \tag{2.97}$$

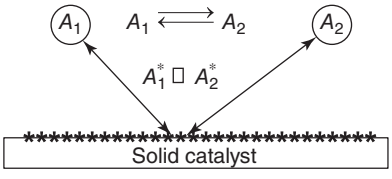

Figure 2.15 Schematic presentation of a catalytic reaction.

$$R_{rx} = r_2 - r_{-2} = k_2 Z_{tot}\theta_1 - k_{-2} Z_{tot}\theta_2 \tag{2.98}$$

$$R_{des} = r_3 - r_{-3} = k_3 Z_{tot}\theta_2 - k_{-1} p_2 Z_{tot}\theta_\nu \tag{2.99}$$

The total concentration of active sites is represented by Z_{tot}, and θ_1, θ_2, θ_ν are the fractions occupied by A_1, A_2 and the fraction of vacant sites, respectively.

In order to derive the overall rate equation of this isomerization reaction, one should know the fraction of the sites occupied by each species, θ_1 and θ_2, which is called *fractional surface coverage*:

$$\theta_i = \frac{Z_i}{Z_{tot}} \tag{2.100}$$

The coverage of a catalyst surface by gaseous molecules at constant temperature depends on the partial pressure of this gas above the surface. The quantitative relationships are called *isotherms*.

2.5.1.1 The Langmuir Adsorption Isotherms

For describing the kinetics of heterogenous catalytic reactions, the *Langmuir adsorption isotherms* are used mainly. We now derive them for associative, dissociative, and competitive adsorption. The main assumptions are the following:

- The solid surface is uniform and contains a number of equivalent sites, each can be occupied by only one species of adsorbate;
- A dynamic equilibrium exists between the gas and the adsorbed molecules at constant temperature and pressure; adsorbate molecules from the gas phase are continually colliding with the surface. If they impact a vacant adsorption site, they may form a bond with the site and stick. If they strike a filled site, they are reflected back into the gas phase;
- Once adsorbed, the molecules are localized
- The enthalpy of adsorption per site remains constant irrespective of coverage (no lateral interaction between the adsorbed species).

When molecules are hitting the surface, they can interact by bonding with an active site being attached for some time. This process can be considered as chemical reaction and are characterized by the rates of adsorption, r_{ads}, and desorptions, r_{des}.

$$\begin{aligned} A_1 + {}^* &\rightarrow A_1^* \quad r_{ads} = k_1 p_1 \theta_\nu \\ A_1^* &\rightarrow A_1 + {}^* \quad r_{des} = k_{-1}\theta_1 \end{aligned} \tag{2.101}$$

When the equilibrium is attained, $r_{des} = r_{ads}$, and after introducing the adsorption equilibrium constant $K_1 = k_1/k_{-1}$, we can write the *Langmuir adsorption isotherm* for associative adsorption of gas A_1 (without any dissociation on interaction with the surface) and only one adsorbing gas present (Example 2.8):

$$\theta_1 = \frac{K_1 \cdot p_1}{1 + K_1 \cdot p_1} \tag{2.102}$$

Example 2.8: Adsorption isotherm.

Determine the fraction of a catalyst surface occupied under equilibrium for a species A_1 at the partial pressure of 1, 2, and 5 bar ($K = 5\,\text{bar}^{-1}$).

Solution:

The amount of surface occupied can be calculated using *Langmuir adsorption isotherms* given by Equation 2.102.

$$\theta_1(p_1 = 1\,\text{bar}) = \frac{K_1 \cdot p_1}{1 + K_1 \cdot p_1} = \frac{5 \cdot 1}{1 + 5 \cdot 1} = 0.83$$

$$\theta_1(p_1 = 2\,\text{bar}) = 0.9$$

$$\theta_1(p_1 = 5\,\text{bar}) = 0.96$$

The common form to present this equation as a linear dependence of $1/\theta_1$ against $1/p_1$ allows to find experimentally the constant of adsorption equilibrium, K_1, and to verify a consistency of the Langmuir assumptions:

$$\frac{1}{\theta_1} = \frac{1}{K_1 \cdot p_1} + 1 \tag{2.103}$$

For dissociative adsorption (when molecules break their bonds on interaction involving two surface sites) the same considerations can be applied leading to the corresponding isotherm:

$$\mathrm{A_2} + 2 * \rightleftharpoons 2\,\mathrm{A_1^*}$$

$$\theta_1 = \frac{\sqrt{K_1 \cdot p_1}}{1 + \sqrt{K_1 \cdot p_1}} \tag{2.104}$$

This is a very important case because molecules like H_2 or O_2 (participating in catalytic hydrogenation and oxidation reactions) often dissociate on the catalytic surface adsorbing with fragmentation. This brings some consequences for the observed kinetics and optimization of the reaction conditions.

Competitive adsorption takes place when two (or more) different molecules are in the gas phase and compete for the same sites. If each species adsorbs on one site only without dissociation, the corresponding Langmuir isotherm is as follows:

$$\theta_i = \frac{K_i p_i}{1 + \sum_i K_i p_i} \tag{2.105}$$

where θ_i is the fractional coverage; K_i, the constant of adsorption equilibrium of molecule A_i.

Data for the isotherm can be obtained experimentally from the equilibrium coverage of the surface at a particular temperature over a range of pressures and then presented in a linear form allowing finding K_i. From the K_i at different temperatures, the heat of adsorption ($\Delta H_{a,i}$) can be estimated using the van't Hoff

equation:

$$K_{i,T_2} = K_{i,T_1} \exp\left(\frac{-\Delta H_{a,i}\left(T_1 - T_2\right)}{RT_1T_2}\right) \tag{2.106}$$

As the adsorption is always exothermic, K_i decreases with temperature.

2.5.1.2 Basic Kinetic Models of Catalytic Heterogenous Reactions

In general, a mechanism for any complex reaction (catalytic or non-catalytic) is defined as a sequence of elementary steps involved in the overall transformation. To determine these steps and especially to find their kinetic parameters is very rare if at all possible. It requires sophisticated spectroscopic methods and/or computational tools. Therefore, a common way to construct a microkinetic model describing the overall transformation rate is to assume a simplified reaction mechanism that is based on experimental findings. Once the model is chosen, a rate expression can be obtained and fitted to the kinetics observed.

Some basic models often used for heterogenous catalytic reactions are described and the overall rate expressions are developed.

Langmuir-Hinshelwood Model The main assumption of this model is that the catalytic reaction proceeds only *via* chemical adsorption of all reactants on the catalytic surface and the transformation takes place as a series of surface reactions ending up with a desorption of the products.

Let's first consider a monomolecular transformation, like the catalytic isomerization of hydrocarbons, as a simple example.

$$A_1 \rightleftharpoons A_2 \tag{2.107}$$

The transformation can be described by considering three surface processes as shown in Equation 2.108: adsorption of the reactant, surface reaction, and desorption of the product. If the reaction is carried out in an open reactor under constant conditions, for example, in a catalytic packed bed reactor, the fractions occupied by A_1 and A_2 are time invariant $\left(\frac{d\theta_1}{dt} = \frac{d\theta_2}{dt} = 0\right)$. With Equations 2.97–2.99 we obtain:

$$\begin{aligned}\frac{d\theta_1}{dt} &= k_1 Z_{tot} p_1 \theta_v - k_{-1} Z_{tot}\theta_1 - k_2 Z_{tot}\theta_1 + k_{-2} Z_{tot}\theta_2 = 0\\ \frac{d\theta_2}{dt} &= k_2 Z_{tot}\theta_1 - k_{-2} Z_{tot}\theta_2 - k_3 Z_{tot}\theta_2 + k_{-3} Z_{tot} p_2 \theta_v = 0\end{aligned} \tag{2.108}$$

As the open reactor operates under stationary conditions, accumulation of products and reactants are excluded. In consequence, the transformation rate of

A_1 corresponds to the production rate of A_2.

$$-R_1 = R_2$$

or

$$-k_1 p_1 \theta_\nu + k_{-1}\theta_1 = k_3\theta_2 - k_{-3} p_2 \theta_\nu \tag{2.109}$$

with

$$\theta_1 + \theta_2 + \theta_\nu = 1 \tag{2.110}$$

We can eliminate the different occupied fractions of active sites and we get finally the dependence of the production rate as function of the partial pressures of A_2 and A_1.

$$R_2 = \frac{kZ_{\text{tot}}(p_1 - p_2/K)}{1 + k_I p_1 + k_{II} p_2} \tag{2.111}$$

With:

$$k = \frac{k_1 k_2 k_3}{k_{-1}(k_{-2} + k_3) + k_2 k_3}$$

$$k_I = \frac{k_1(k_2 + k_{-2} + k_3)}{k_{-1}(k_{-2} + k_3) + k_2 k_3}$$

$$k_{II} = \frac{k_{-3}(k_{-1} + k_2 + k_{-2})}{k_{-1}(k_{-2} + k_3) + k_2 k_3}$$

$$K = \frac{k_1 k_2 k_3}{k_{-1} k_{-2} k_{-3}} \tag{2.112}$$

It is evident that the six individual rate constants cannot be obtained under steady-state reaction conditions. To estimate their values, independent measures of the adsorption and reaction behavior under transient (non-steady-state) conditions are necessary.

The Quasi-Surface Equilibrium Approximation If we suppose that the adsorption and desorption processes are fast compared to the surface reaction, we can estimate the surface concentrations from the equilibrium constants. With the Langmuir adsorption isotherm, the following relations result for the simple monomolecular reaction presented in Equation 2.107.

$$\theta_1 = \frac{K_1 p_1}{1 + K_1 p_1 + K_2 p_2}$$

$$\theta_2 = \frac{K_2 p_2}{1 + K_1 p_1 + K_2 p_2}$$

$$\text{with}: K_1 \simeq \frac{k_1}{k_{-1}}; K_2 \simeq \frac{k_2}{k_{-2}} \tag{2.113}$$

The transformation rate is then simply given by:

$$-R_1 = k_2 Z_{\text{tot}} \theta_1 - k_{-2} Z_{\text{tot}} \theta_2 = \frac{k_2 Z_{\text{tot}} K_1 \left(p_1 - p_2/K_{\text{eq}}\right)}{1 + K_1 p_1 + K_2 p_2},\ K_{\text{eq}} = \frac{k_2}{k_{-2}} \frac{K_1}{K_2} \quad (2.114)$$

For a quasi-irreversible reaction and negligible product adsorption ($K_{\text{eq}} \rightarrow \infty, K_2 \ll K_1$), Equation 2.114 is further simplified to give:

$$-R_1 = \frac{k_2 Z_{\text{tot}} K_1 p_1}{1 + K_1 p_1} \quad (2.115)$$

If we divide denominator and nominator by K_1 we obtain the Michaelis–Menten equation, where K_M corresponds to $1/K_1$.

The Most Abundant Surface Intermediate (MASI) Approximation Catalytic transformations may include the formation of many intermediates on the catalyst surface, which are difficult to identify. In these cases, it is impossible to formulate a kinetic model based on all elementary steps. Often, one of the intermediates adsorbs much more strongly in comparison to the other surface species, thus occupying nearly all active sites. This intermediate is called the *most abundant surface intermediate "masi"* [24]. For a simple monomolecular reaction, $A_1 \rightarrow A_2$, the situation can be illustrated with the following scheme:

$$\begin{aligned}
&A_1 + {}^* \xrightarrow{k_1} A_1^* \\
&A_1^* \xrightarrow{k_2} I_2^* \\
&\quad\vdots \\
&I_{n-1}^* \xrightarrow{k_{n-1}} I_n^* \text{ (masi)} \\
&I_n^* \xrightarrow{k_n} A_2 + {}^*
\end{aligned} \quad (2.116)$$

Neglecting all intermediates having a very short lifetime on the catalyst results in:

$$\theta_v + \theta_{\text{masi}} \simeq 1 \quad (2.117)$$

The transformation rate of reactant A_1 corresponds to the first step in Equation 2.116:

$$-R_1 = k_1 Z_{\text{tot}} p_1 \theta_v = k_1 Z_{\text{tot}} p_1 (1 - \theta_{\text{masi}}) \quad (2.118)$$

The final product is formed in the nth step and corresponds to the transformation to A_2 and its desorption:

$$R_2 = k_n Z_{\text{tot}} \theta_{\text{masi}} \quad (2.119)$$

As steady state holds, $R_2 = -R_1$, and θ_v can be easily calculated and the final expression for describing the production rate is given by:

$$R_2 = \frac{k_1 Z_{\text{tot}} p_1}{1 + K p_1}; \text{with } K = \frac{k_1}{k_n} \quad (2.120)$$

It is important to underline that the mathematical form of the obtained kinetic equations (Equations 2.111, 2.114, and 2.120) are quite similar, whereas the interpretation of the corresponding model parameters and the physical meaning of the constants are very different.

Bimolecular Catalytic Reactions Supposing that the surface reaction is the rate-determining step, we obtain for an irreversible bimolecular reaction the following relations:

$$A_1 + A_2 \rightarrow A_3$$
$$-R_1 = kZ_{\text{tot}}\theta_1\theta_2 \tag{2.121}$$

The surface fractions occupied by the reactants A_1 and A_2 are given by the Langmuir isotherm, supposing competitive adsorption and neglecting the coverage by the product.

$$\theta_1 = \frac{K_1 p_1}{1 + K_1 p_1 + K_2 p_2}$$

$$\theta_2 = \frac{K_2 p_2}{1 + K_1 p_1 + K_2 p_2}$$

$$\theta_3 \simeq 0 \tag{2.122}$$
$$-R_1 = R_3 = k_3 \cdot Z_{\text{tot}}\theta_1 \cdot \theta_2 = \frac{k_3 \cdot Z_{\text{tot}} K_1 p_1 \cdot K_2 p_2}{(1 + K_1 p_1 + K_2 p_2)^2} \tag{2.123}$$

At constant pressure of the reaction partner A_2, the transformation rate as function of p_1 passes through a maximum (demonstrated in Example 2.9). The maximum depends on p_2 and the values of the adsorption constants K_1 and K_2. The optimum pressure for A_1 can easily be calculated with Equation 2.124.

$$p_{1,\text{op}} = \frac{1 + K_2 p_2}{K_1} \tag{2.124}$$

Example 2.9: Maximum rate of bimolecular catalytic reaction.

Investigate the surface coverage and normalized transformation rate ($R_1/R_{1,\,\text{max}}$) as a function of the mole fraction of A_1 for a reaction given by Equation 2.121. The constants are $K_1 = 2\,\text{bar}^{-1}$ and $K_2 = 3\,\text{bar}^{-1}$ while $p_2 = 1\,\text{bar}$.

Solution:

The transformation rate is maximal for $\theta_1 = \theta_2$. The surface coverage θ_1 and θ_2 can be calculated using Equation 2.122. To calculate the unknown p_1, the mole fraction, $y_1 = p_1/(p_1 + p_2)$, in the range of 0–1 can be assumed. The transformation rate is given by Equation 2.121. However, we have to also calculate

the maximum transformation rate $R_{1,\,max}$. As the R_1 is directly proportional to product $\theta_1\theta_2$, the maximum rate can be achieved when the product is maximum. Thus,

$$\frac{R_1}{R_{1,\max}} = \frac{\theta_1\theta_2}{\theta_1^2} \tag{2.125}$$

The results are illustrated in Figure 2.16.

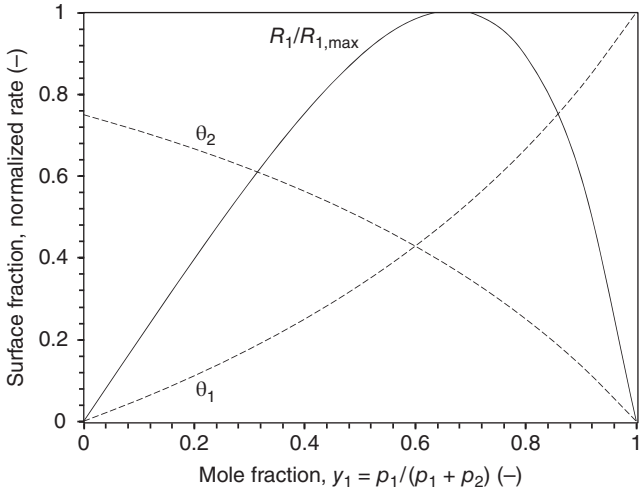

Figure 2.16 Surface coverage of A_1 and A_2 and the normalized transformation rate as function of the mole fraction of A_1.

2.5.2
Deactivation of Heterogenous Catalysts

In heterogenous catalytic reactions, a decrease in catalyst activity is often observed with increasing operation time. There are many reasons for this; the most important factors can be classified into three groups:

- Poisoning of the catalyst surface by irreversible adsorption and/or reaction of a chemical species, thus making the active centers required for the catalyzed reaction inactive. Example is CO adsorption on iron catalysts used for the ammonia synthesis.
- Coverage of the surface with substances that leads to a mechanical blockage of the catalytically active surface. Example is deposition of coke in various hydrocarbon reactions such as isomerization, cyclization, and cracking.

- Decreasing of the active surface by sintering and recrystallization processes. Example is the decrease of the active nickel surfaces through recrystallization on alumina-supported nickel catalysts in hydrogenation reactions.

For the course of a catalytic reaction whose kinetics can be described as:

$$r = \frac{k_r' Z_{\text{tot}} K_1 p_1}{1 + K_1 p_1} = \frac{k_1 p_1}{1 + K_1 p_1} \tag{2.126}$$

the number Z_{tot} of active surface sites can decrease with the operating time (also known as *lifetime*) t' of the catalyst, for example, by poisoning through components present in the system that do not take part in the reaction. The decreasing catalyst activity can be taken into account in the kinetic model by introducing an activity factor, $a(t')$, which is a function of the operation time t'.

$$a(t') = \frac{k_r(t')}{k_r(t' = 0)} \tag{2.127}$$

Thus, the activity factor corresponds to the ratio between the rate constant after a certain time of operation referred and the initial value. It is important to underline that this way of including the deactivation is possible only if the deactivation kinetics is separable from the transformation kinetics, viz. the kinetic model for the transformation is not altered by the deactivation process.

In the present case, the rate of deactivation r_d corresponds to the change in the number of active surface sites with time of operation. The rate constants for catalysts undergoing deactivation can be formulated as follows:

$$k_r(t') = k_r(t' = 0) \cdot a(t'). \tag{2.128}$$

The rate of deactivation can depend on the temperature, the activity factor $a(t')$ of the catalyst, the concentration of a component c_{dea} (causing deactivation), and on the activation energy E_d of the deactivation process.

$$-r_d = k_d^0 e^{\left(-\frac{E_d}{RT}\right)} f(a, c_{\text{dea}}) \tag{2.129}$$

If the deactivation process is slow compared to the rate of transformation, the activity is quasi uniform in the reactor and Equation 2.129 can be formulated simply as a power term, and we obtain

$$-r_d = -\frac{\mathrm{d}a}{\mathrm{d}t'} = k_d a^n c_{\text{dea}}^m. \tag{2.130}$$

For the case that $m = 0$, that is, there are no poisoning components in the reaction mixture but rather a sintering process is the cause of the deactivation, and $n = 1$, then Equation 2.129 simplifies to

$$-r_d = k_d^0 e^{\left(-\frac{E_d}{RT}\right)} a \tag{2.131}$$

If under the intrinsic conditions (without transport disguises) of a catalytic process, r_d depends only on c_{dea}, the poisoning may be supposed to be the main cause of deactivation. For more complex situations, like in the case of fast deactivation, "a" becomes not only a function of time but also a function of location within

an eventual reactor. For detailed studies on deactivation kinetics, the reader is referred to [25, 26].

2.6
Mass and Heat Transfer Effects on Heterogenous Catalytic Reactions

Heterogenous catalytic reactions involve by their nature a combination of reaction and transport processes, as the reactants must be first transferred from the bulk of the fluid phase to the catalyst surface, where the reaction occurs. The combined reaction and transport processes are shown schematically in Figure 2.17. We suppose a porous catalyst particle with a large specific surface area surrounded by liquid or gaseous reaction mixture.

For the transformation of the reactant A_1 to the product A_2, the following steps are necessary:

1) external diffusion of reactants (film diffusion)
2) internal diffusion of reactants (pore diffusion)
3) adsorption of the reactants on the surface
4) catalytic reaction on the surface
5) desorption of the products
6) internal diffusion of products (pore diffusion)
7) external diffusion of products (film diffusion).

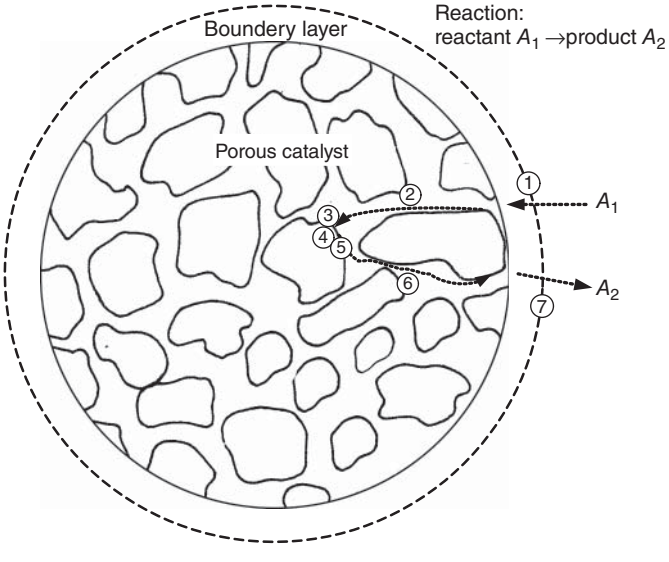

Figure 2.17 Physical and chemical steps involved in heterogenous catalytic reactions. (Adapted from Ref. [16], Figure 4.1 Copyright © 2012, Wiley-VCH GmbH & Co. KGaA.)

If the rates of the chemical steps 3–5 are comparable or higher than the transport processes 1, 2 and 6, 7, significant concentration profiles of A_1 and A_2 inside the catalyst particle or in the surrounding layer will occur. If the intrinsic rates are very high as compared to the diffusion process in the pores, the reaction will take place only near the external surface, and the observed transformation rate will be controlled by the external mass transfer. The same situation is observed for nonporous pellets or so-called "egg-shell" catalysts, where the active phase is placed in a layer near the outer pellet surface. If the intrinsic reaction rate is comparable with the diffusion rate within the pores, a pronounced concentration profile of the reactant A_1 within the pellet will develop.

Simultaneously to the chemical transformation, heat is released or consumed in the case of exothermic or endothermic reactions. Consequently, temperature gradients inside and outside of the catalyst pellet will develop. The different situations are illustrated in Figure 2.18.

As a consequence of the concentration profiles caused by the transfer phenomena, the observed (effective) reaction rates are modified compared to the rate, which would occur at constant bulk phase concentration. This effect is commonly characterized by an effectiveness factor as defined in Equation 2.132:

$$\eta_{ov} = \frac{\text{observed rate of reaction}}{\text{rate of reaction at bulk concentration and temperature}} \tag{2.132}$$

Besides the modification of the overall reaction rate, the product selectivity may be changed. This is discussed in detail in the following subsections.

2.6.1 External Mass and Heat Transfer

The first step in heterogenous catalytic processes is the transfer of the reactant from the bulk phase to the external surface of the catalyst pellet. If a nonporous catalyst is used, only external mass and heat transfer can influence the effective rate of transformation. The same situation will occur for very fast reactions, where the reactants are completely consumed at the external catalyst surface. As no internal mass and heat transfer resistances are considered, the overall catalyst effectiveness factor corresponds to the external effectiveness factor, η_{ex}. For a simple irreversible reaction of nth order, the following relation results:

$$\eta_{ov} = \eta_{ex} = \frac{k(T_s) \cdot c_{i,s}^n}{k(T_b) \cdot c_{i,b}^n} = \frac{k(T_s)}{k(T_b)} \left(\frac{c_{i,s}}{c_{i,b}} \right)^n \tag{2.133}$$

2.6.1.1 Isothermal Pellet

The external mass transfer process can be described by the so-called film model as shown in Figure 2.19. According to the film model, a stagnant fluid layer of thickness δ surrounds the external surface, where the total resistance to mass transfer is located. Accordingly, the concentration profile is confined to this layer. The molar flux of reactant A_i is proportional to the difference in concentration (the driving

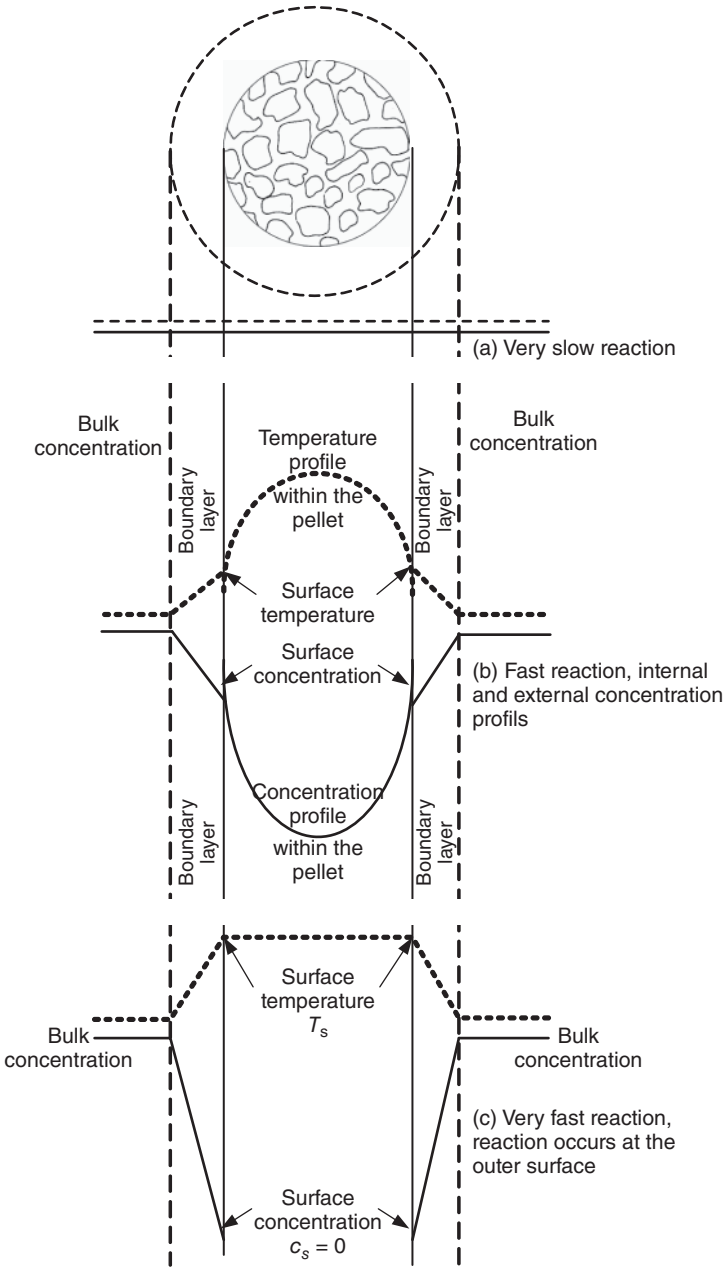

Figure 2.18 Concentration profiles in porous catalysts for different reaction regimes. (Adapted from Ref. [16], Figure 4.5 Copyright © 2012, Wiley-VCH GmbH & Co. KGaA.)

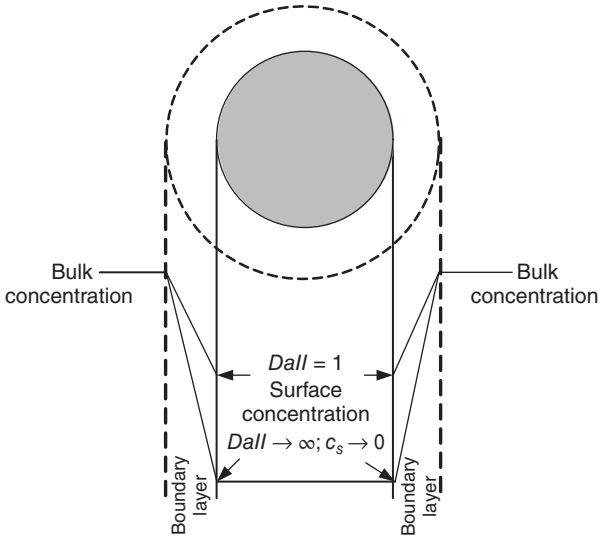

Figure 2.19 External concentration profile according to the film model. (Adapted from Ref. [16], Figure 4.6 Copyright © 2012, Wiley-VCH GmbH & Co. KGaA.)

force) as given in Equation 2.134.

$$J_i = k_m(c_{i,b} - c_{i,s}) \tag{2.134}$$

with k_m the mass transfer coefficient and $c_{i,s}$, $c_{i,b}$ the concentration of A_i at the external surface and the bulk of the fluid, respectively. At steady-state condition, the molar flux of A_i is equal to the rate of transformation at the outer catalyst surface:

$$J_i = k_m(c_{i,b} - c_{i,s}) = -R_{i,p} \cdot \frac{V_p}{A_p} = \frac{-R_{i,p}}{a_p};$$

$$\text{with } R_{i,p} = \nu_i r_p \tag{2.135}$$

where R_i is the transformation rate of A_i, per volume of catalyst pellet, r_p, the intrinsic reaction rate, $V_{p,}$, A_p the pellet volume and outer surface, respectively, and a_p the specific external surface area of the pellet.

$$a_p = \frac{A_p}{V_p}; a_p = \frac{6}{d_p} \text{ (sphere)} \tag{2.136}$$

For an irreversible first order surface reaction with $\nu_1 = -1$, we obtain for the reactant A_1:

$$J_1 = k_m(c_{1,b} - c_{1,s}) = \frac{-R_{1,p}}{a_p} = \frac{k_r c_{1,s}}{a_p} \tag{2.137}$$

The reactant concentration on the surface is given by:

$$c_{1,s} = \frac{k_m a_p}{k_m a_p + k_r} \cdot c_{1,b} \tag{2.138}$$

and for the effective (observed) transformation rate follows:

$$-R_{1,\text{eff}} = k_r \frac{k_m a_p}{k_m a_p + k_r} \cdot c_{1,b} \tag{2.139}$$

A similar development can be observed for irreversible *n*th order reactions. At steady state follows:

$$k_m a_p (c_{1,b} - c_{1,s}) = -R_{1,p} = k_r c_{1,s}^n \tag{2.140}$$

Dividing by $k_m a_p c_{1,b}$ leads to

$$1 - \frac{c_{1,s}}{c_{1,b}} = \frac{k_r c_{1,b}^{n-1}}{k_m a_p} \left(\frac{c_{1,s}}{c_{1,b}}\right)^n = DaII \left(\frac{c_{1,s}}{c_{1,b}}\right)^n \tag{2.141}$$

The second Damköhler number, *DaII*, is defined as the ratio between the characteristic mass transfer time $t_m = 1/(k_m a_p)$ and the characteristic reaction time, $t_r = 1/(k_r c_{1,b}^{n-1})$.

$$DaII = \frac{t_m}{t_r} = \frac{k_r c_{1,b}^{n-1}}{k_m a_p} \tag{2.142}$$

With Equation 2.133 we find for the external effectiveness under isothermal conditions:

$$\eta_{\text{ex}} = \left(\frac{c_{1,s}}{c_{1,b}}\right)^n \tag{2.143}$$

The external effectiveness factors as function of the second Damköhler number are obtained by solving Equation 2.141. This is done for reaction orders $n = 1$, 2, $^1/_2$, and -1 and displayed in Figure 2.20 [27].

$$n = 1: \quad \eta_{\text{ex}} = \frac{1}{1 + DaII}$$

$$n = 2: \quad \eta_{\text{ex}} = \left(\frac{\sqrt{1 + 4\,DaII} - 1}{2\,DaII}\right)^2$$

$$n = \frac{1}{2}: \quad \eta_{\text{ex}} = \left[\frac{2 + DaII^2}{2}\left(1 - \sqrt{1 - \frac{4}{(2 + DaII^2)^2}}\right)\right]^{\frac{1}{2}}$$

$$n = -1: \eta_{\text{ex}} = \frac{2}{1 + \sqrt{1 - 4\,DaII}}; \text{for } DaII < 0.25 \tag{2.144}$$

From Figure 2.20 we see that

- The effectiveness factor diminishes for the same *DaII* with increasing reaction order
- An effectiveness factor higher than one is obtained for reaction with reactant inhibition (negative reaction order)

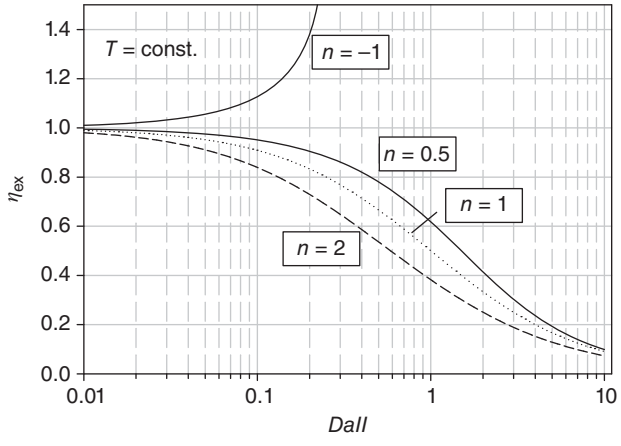

Figure 2.20 Isothermal external effectiveness factor as function of the Damköhler number. (Adapted from Ref. [16], Figure 4.7 Copyright © 2012, Wiley-VCH GmbH & Co. KGaA.)

- For large values of *DaII* the effectiveness is inversely proportional to *DaII* ($\eta_{ex} \simeq 1/DaII$) for all reactions with positive reaction order.

The observed reaction rate is given by:

$$r_{p,\text{eff}} = k_{\text{eff}} c_{1,b}^{n'} = \eta_{ex} k_r c_{1,b}^{n} \tag{2.145}$$

With increasing intrinsic reaction rate (increasing *DaII*) the observed rate constant approaches the volumetric mass transfer coefficient ($k_{\text{eff}} \rightarrow k_m a_p$) and the reaction order changes from n to unity.

Whereas Figure 2.20 is quite instructive, it is not of practical use for estimating the importance of the mass transfer influence from experimental data, as the intrinsic rate constant is normally unknown. Replotting the effectiveness factor as function of the ratio between observed reaction rate to the maximum mass transfer rate called as *Carberry number* (*Ca*) allows estimating the external effectiveness factor plotted in Figure 2.21.

$$\frac{r_{p,\text{eff}}}{k_m a_p c_{1,b}} = \eta_{ex} \frac{k_r c_{1,b}^{n-1}}{k_m a_p} = \eta_{ex} DaII = Ca \tag{2.146}$$

Isothermal Yield and Selectivity For a network of parallel and/or consecutive reactions mass transfer may affect drastically the target product yield. For consecutive first order reactions and in the absence of mass transfer influence we obtain for the transformation rate of the reactant and the production rate of the intermediate (the target product):

$$A_1 \xrightarrow{k_1} A_2 \xrightarrow{k_2} A_3 \tag{2.147}$$

$$-R_1 = k_1 c_{1,b}$$

$$R_2 = k_1 c_{1,b} - k_2 c_{2,b} \tag{2.148}$$

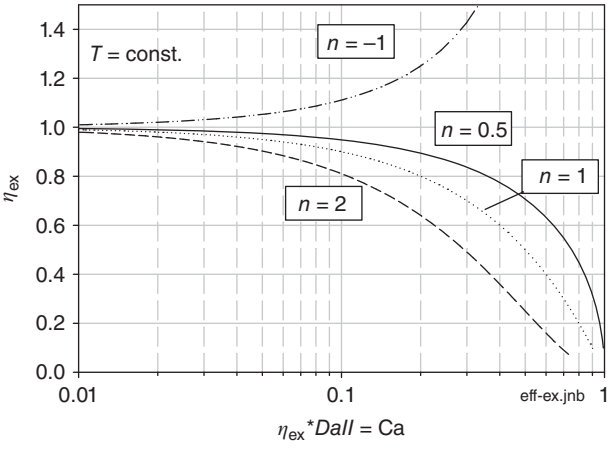

Figure 2.21 Effectiveness factor as function of the observable variable: the Carberry number (Adapted from Ref. [15], Figure 4.8 Copyright © 2012, Wiley-VCH GmbH & Co. KGaA)

The instantaneous or point selectivity for the intermediate product is obtained by dividing R_2 by $(-R_1)$:

$$s_{2,1} = -\frac{R_2}{R_1} = 1 - \frac{k_2 c_{2,b}}{k_1 c_{1,b}},\ |\nu_1| = |\nu_2| = 1 \tag{2.149}$$

Anticipating the mass transfer phenomena in the extreme case results in:

$$k_m a_p (c_{1,b} - c_{1,s}) = k_1 c_{1,s} \tag{2.150}$$

$$k_m a_p (c_{2,s} - c_{2,b}) = k_1 c_{1,s} - k_2 c_{2,s} \tag{2.151}$$

Solving for the surface concentrations $c_{1,s}$ and $c_{2,s}$ we obtain for the instantaneous selectivity the following relations:

$$(s_{2,1})_{\text{eff}} = -\frac{R_{2,s}}{R_{1,s}} = 1 - \frac{k_2 c_{2,s}}{k_1 c_{1,s}}$$
$$(s_{2,1})_{\text{eff}} = \frac{1}{1 + DaII_2} - \frac{k_2}{k_1}\frac{(1 + DaII_1)}{(1 + DaII_2)}\frac{c_{2,b}}{c_{1,b}} \tag{2.152}$$

with $DaII_1 = k_1/(k_m a_p)$ and $DaII_2 = k_2/(k_m a_p)$.

Under the initial conditions at the reactor entrance the product concentrations are zero and the instantaneous selectivity becomes:

$$(s_{2,1})_{\text{eff},0} = \frac{1}{1 + DaII_2} = \frac{1}{1 + (k_2/k_m a_p)} \tag{2.153}$$

Obviously, the effective selectivity of the intermediate product depends on the ratio of the escape rate from the surface to its rate of the transformation to the consecutive product A_3 on the catalytic surface. Low mass transfer rates as compared to the rate of the consecutive reaction is detrimental for the selectivity and

yield of the intermediate product. At contrast, high mass transfer rates ($k_m \gg k_2$) increase the initial selectivity of the intermediate product approaching unity.

For parallel reactions the influence of mass transfer depends on the individual reaction orders:

$$A_1 \xrightarrow{k1} A_2;\ R_2 = k_1 c_{n_1-1} \tag{2.154}$$

$$A_1 \xrightarrow{k2} A_3;\ R_3 = k_2 c_{n_2-1} \tag{2.155}$$

The ratio between the products A_2 and A_3 depends on the rate constants and the reactant concentration.

$$\frac{R_2}{R_3} = \frac{k_1}{k_2} c_1^{(n_1-n_2)} \tag{2.156}$$

As the concentration gradient around the catalyst leads to a lower surface concentration compared to the bulk, the observed alteration of rate ratio depends on the individual reaction order:

$$\frac{(R_{2,s}/R_{3,s})}{(R_{2.b}/R_{3,b})} = \left(\frac{c_{1,s}}{c_{1,b}}\right)^{(n_1-n_2)} \tag{2.157}$$

As $c_{1,\,s} < c_{1,\,b}$ we see that diffusion intrusion leads to

- a reduced selectivity for A_2, if $n_1 > n_2$
- an increased selectivity for A_2, if $n_1 < n_2$
- no change of the selectivity for $n_1 = n_2$.

Nonisothermal Pellet For highly endothermic or exothermic reactions, the temperature of the catalyst surface can be considerably different from the temperature of the surrounding fluid.

We evaluate the surface temperature by the heat balance at steady state conditions:

$$(-\Delta H_r) \cdot r_{p,\text{eff}} = h \cdot a_p (T_s - T_b) \tag{2.158}$$

with h, the heat transfer coefficient.

We divide Equation 2.158 by $k_m a_p c_{1,b}$

$$\frac{h \cdot a_p}{k_m a_p c_{1,b}} (T_s - T_b) = (-\Delta H_r) \cdot \frac{r_{p,\text{eff}}}{k_m a_p c_{1,b}}$$

or

$$\frac{h \cdot a_p}{k_m a_p c_{1,b}} (T_s - T_b) = (-\Delta H_r) \cdot \eta_{\text{ex}} DaII = (-\Delta H_r) \cdot Ca \tag{2.159}$$

Invoking Chilton-Colburn analogy between heat and mass transfer:

$$\frac{h}{\rho \cdot c_p} Pr^{2/3} = k_m Sc^{2/3} \tag{2.160}$$

we obtain the ratio between heat and mass transfer coefficient:

$$\frac{h}{k_m} = \rho c_p \left(\frac{Sc}{Pr}\right)^{2/3} \tag{2.161}$$

and finally with Equation 2.159:

$$T_s = T_b + \Delta T_{\text{ad}} \left(\frac{Pr}{Sc}\right)^{2/3} Ca$$

$$\frac{T_s}{T_b} = 1 + \frac{\Delta T_{\text{ad}}}{T_b} \left(\frac{Pr}{Sc}\right)^{2/3} Ca = 1 + \beta_{\text{ex}} \cdot Ca \tag{2.162}$$

With $\Delta T_{\text{ad}} = \frac{(-\Delta H_r) c_{1,b}}{\rho c_p}$ the adiabatic temperature rise, $Pr = \frac{\nu}{\alpha} = \frac{\nu}{\lambda/(\rho c_p)}$ the Prandtl number, and $Sc = \frac{\nu}{D_m}$ the Schmidt number.

For a given system the temperature difference between bulk and surface depends on the reactant concentration via ΔT_{ad}, the ratio between Prandtl and Schmidt number, and the Carberry number. The temperature difference is maximum for reactions limited by mass transfer ($Ca = > 1$). As for gases the Schmidt and Prandtl numbers are approximately unity ($Pr \simeq Sc \simeq 1$), the temperature difference can reach the adiabatic temperature ($T_s - T_b \simeq \Delta T_{\text{ad}}$).

The nonisothermal external effectiveness factor is

$$\eta_{\text{ex}} = \frac{r_{p,\text{eff}}}{r_{p,b}} = \frac{k(T_s)}{k(T_b)} \left(\frac{c_{1,s}}{c_{1,b}}\right)^n \tag{2.163}$$

On the basis of Equations 2.143 and 2.144 we can estimate the surface concentration and obtain for a first order reaction: $c_{1,s}/c_{1,b} = (1 + DaII)^{-1}$.

The rate constant at the surface temperature, $k(T_s)$, is given by the Arrhenius law:

$$k(T_s) = k(T_b) \exp\left(-\frac{E}{RT_b}\left(\frac{T_b}{T_s} - 1\right)\right) = k(T_b) \exp\left(-\gamma\left(\frac{T_b}{T_s} - 1\right)\right) \tag{2.164}$$

with $\gamma = \frac{E}{RT_b}$, the Arrhenius number. The surface temperature is determined by the adiabatic temperature rise and the ratio of Schmidt and Prandtl number as shown in Equation 2.162. In summary, the external effectiveness factor for a given Ca depends on the Arrhenius number, γ and the parameter $\beta_{\text{ex}} = \frac{\Delta T_{\text{ad}}}{T_b}\left(\frac{Pr}{Sc}\right)^{2/3}$.

The nonisothermal effectiveness as function of the Ca for different Arrhenius numbers and β_{ex} are shown in Figures 2.22 and 2.23.

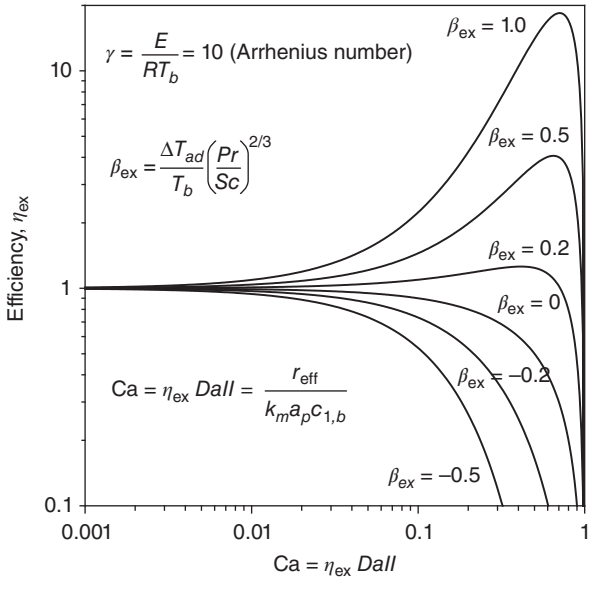

Figure 2.22 Nonisothermal external effectiveness factor as function of the parameter β_{ex} and the Carberry number ($\gamma = 10$). (Adapted from Ref. [16], Figure 4.9 Copyright © 2012, Wiley-VCH GmbH & Co. KGaA.)

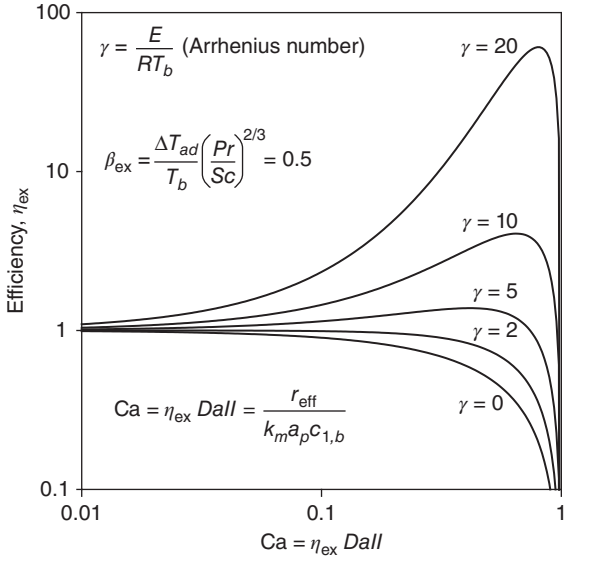

Figure 2.23 Nonisothermal external effectiveness factor as function of the Arrhenius number, γ and the Carberry number ($\beta_{ex} = 0.5$). (Adapted from Ref. [16], Figure 4.10 Copyright © 2012, Wiley-VCH GmbH & Co. KGaA.)

We see that

- the effectiveness factor can be greater than unity for exothermic reactions
- the Arrhenius number γ is more important than the parameter β_{ex} in determining η_{ex}.
- at high values of Carberry number the effectiveness factor falls well below unity even for highly exothermic reactions.

2.6.2 Internal Mass and Heat Transfer

For most catalytic processes, porous catalysts with a high inner specific surface area are used. Therefore, the reactant has to be transported through the pores to the catalytically active sites as described in Figure 2.17. Because of the chemical reaction, a gradient of the reactant concentration in the fluid (gas or liquid) may develop from the outside to the center of the pellet. For the following discussion we assume isotropic particles and that the transport process can be represented by molecular diffusion. The molar flux of reactant A_1 can be described by:

$$J_1 = -D_e \frac{dc_1}{dz} \tag{2.165}$$

where D_e is the effective diffusion coefficient for reactant A_1, and z is the particle coordinate, defined as the distance from the center. Formally, Equation 2.165 corresponds to first Fick's law. As the diffusion occurs within a porous media, an effective diffusion coefficient is introduced. The effective diffusion coefficient takes into account that pores occupy only fraction, ε_p, of the particle volume, and that the pores are not linear in z-direction. As a consequence, the diffusion path through the pores is longer than z. This is accounted for by introducing a tortuosity factor τ_p. With both corrections the effective diffusion coefficient can be estimated with the following expression:

$$D_e = D_1 \frac{\varepsilon_p}{\tau_p} \tag{2.166}$$

with D_1, the molecular diffusion coefficient of reactant A_1.

The particle porosity is in the order of $0.3 < \varepsilon_p < 0.6$, and the tortuosity is found to be in the range of $2 < \tau_p < 5$.

2.6.2.1 Isothermal Pellet

To illustrate the simultaneous diffusion/reaction processes occurring in a porous catalyst, we consider a catalyst in the form of a flat slab of semi-infinite dimension on the outer surface, and of a half thickness L as shown in Figure 2.24.

An irreversible, first order reaction takes place in the porous matrix. The mass-transport is represented by a molecular diffusion. A steady-state mass balance over a differential volume element yields:

$$D_e \frac{dc_1}{dz} - (-R_1) = 0 \tag{2.167}$$

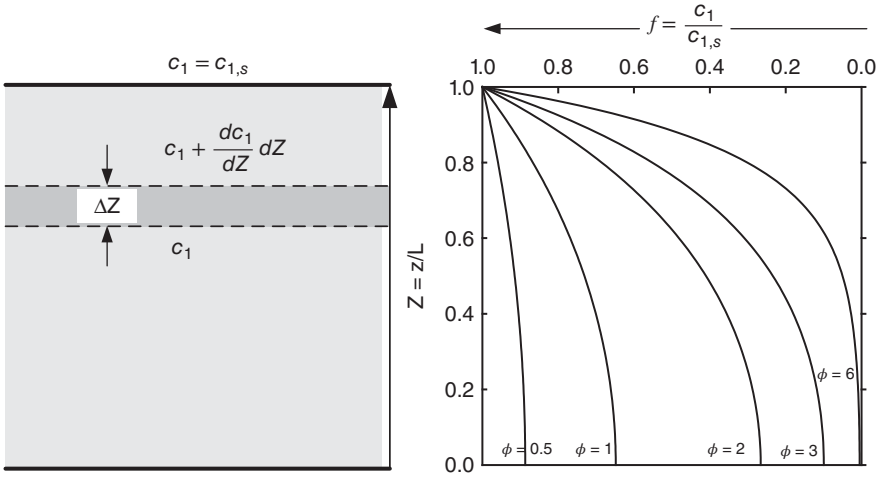

Figure 2.24 (a,b) Diffusion and reaction in a semi-infinite flat slab. (Adapted from Ref. [15], Figure 4.11 Copyright © 2012, Wiley-VCH GmbH & Co. KGaA.)

The boundary conditions define the concentration on the outer surface and have symmetry at the slab center.

$$z = L : c_1 = c_{1,s};\ z = 0 :\ \frac{\mathrm{d}c_1}{\mathrm{d}z} = 0 \tag{2.168}$$

For first order kinetics with $-R_1 = k\, c_1$ Equation 2.167 can be rewritten in a nondimensional form as follows:

$$\frac{\mathrm{d}^2 f}{\mathrm{d}Z^2} - L^2 \left(\frac{k_r}{D_e}\right) f = 0 \tag{2.169}$$

with $f = \frac{c_1}{c_{1,s}}; Z = \frac{z}{L}$.

The group $L^2 \frac{k_r}{D_e}$ corresponds to the ratio between the characteristic diffusion time t_D in the slab and the characteristic reaction time. This ratio is commonly called *Thiele modulus*, φ.

$$\varphi^2 = \frac{t_D}{t_r} = \frac{L^2}{D_e} k; \varphi = L\sqrt{\frac{k_r}{D_e}};\ \text{first order reaction} \tag{2.170}$$

The solution of Equation 2.169 for the concentration profile in the slab is:

$$f = \frac{c_1}{c_{1,s}} = \frac{\cosh(\varphi Z)}{\cosh(\varphi)} \tag{2.171}$$

The effective rate of reaction corresponds to the molar flux at the external surface $J_{1,L}$. Using the concentration profile evaluated for $Z = 1$ from Equation 2.171 we obtain.

$$J_{1,L} = -D_e \left(\frac{\mathrm{d}c_1}{\mathrm{d}z}\right)_{z=L} \tag{2.172}$$

which results in an effective reaction rate per external area of:

$$J_{1,\text{eff}} = \frac{D_e c_{1,s}}{L} \varphi \tanh(\varphi) \tag{2.173}$$

The overall reaction rate per external area in the absence of an internal concentration profile is $J_{1,s} = k_r c_{1,s} L$. From Equation 2.132, the effectiveness factor in the porous catalyst, $\eta_{p,}$ is as follows:

$$\eta_p = \frac{J_{1,\text{eff}}}{J_{1,s}} = \frac{D_e c_{1,s}/L \cdot \varphi \tanh(\varphi)}{k_r c_{1,s} L} = \frac{\tanh \varphi}{\varphi} \tag{2.174}$$

The effective transformation rate per volume of the catalyst is then given by

$$-R_{1,\text{eff}} = \eta_p k_r c_{1,s} = \frac{\tanh \varphi}{\varphi} k_r c_{1,s} \tag{2.175}$$

If the influence of internal diffusion is big ($L^2/D_\text{e} \gg k_\text{r}$), the Thiele modulus becomes large and tanh $\varphi =>$ unity. Therefore, the effectiveness factor for strong diffusional resistances is

$$\eta_p \simeq \frac{1}{\varphi} \tag{2.176}$$

Concentration profiles in slabs for different values of φ are shown in Figure 2.24b.

The results presented above are specific for a first order reaction and a catalyst in the form of a slab. For spherical particles the corresponding equation is

$$\eta_p = \frac{3}{\varphi_s} \left[\frac{1}{\tanh \varphi_s} - \frac{1}{\varphi_s} \right] \tag{2.177}$$

The corresponding solution for a cylinder is

$$\eta_p = \frac{2}{\varphi_c} \frac{I_1(\varphi_c)}{I_0(\varphi_c)} \tag{2.178}$$

where $I_1(\varphi)$ and $I_0(\varphi)$ denote the modified Bessel functions of first and zero order, respectively.

In Figure 2.25 the effectiveness factor as function of the Thiele modulus for different pellet shapes is shown. For small values of the Thiele modulus the effectiveness factor reaches unity in all cases. The reaction rate is controlled by the intrinsic kinetics, and the reactant concentration within the pellet is identical to the concentration at the outer pellet surface. This situation may be observed for low catalyst activity or very small particles as used in fluidized beds or suspension reactors. For large values of the Thiele modulus the dependency of η_p approaches an asymptotic solution: $\eta_p = m/\varphi$ with $m = 1, 2, 3$ for a slab, a cylinder, and a sphere, respectively. This situation may occur for very fast reactions or large catalyst particles. The concentration in the center of the catalyst particles approaches zero for $\eta_p < 0.2$.

The observation that the slope of the asymptotic solution for $\eta(\varphi)$ becomes independent of the particle geometry suggests that the dependence of the effectiveness factor on the Thiele modulus can be described by a generalized relationship, valid

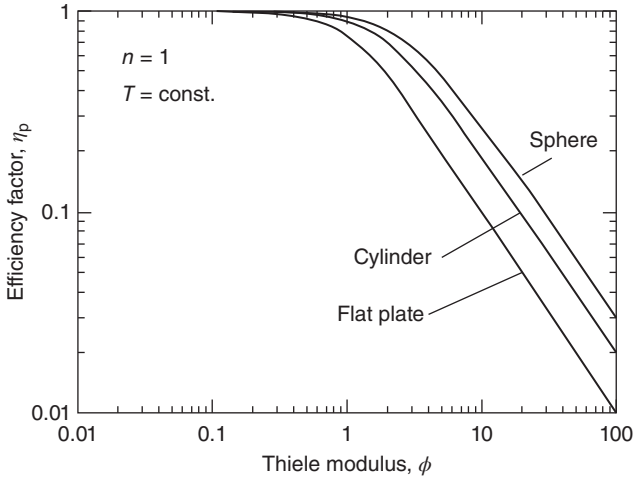

Figure 2.25 Effectiveness factor as function of the Thiele modulus for different pellet shapes. (Adapted from Ref. [28], Figure 5 Copyright © 2008, Wiley-VCH GmbH & Co. KGaA.)

for arbitrary pellet shapes. This was in fact demonstrated by Aris [29] by defining a general Thiele modulus φ_{gen} based on the ratio of pellet volume to external surface as characteristic diffusion length. A further correction was proposed by Petersen to get a general effectiveness factor for a *n*th order reaction with a characteristic reaction time $t_r = (k_r c_{1,s}^{(n-1)})^{-1}$. The final definition is given in Equation 2.179.

$$\varphi_{\text{gen}} = \frac{V_p}{A_p}\sqrt{\frac{k_r c_{1,s}^{(n-1)}}{D_e}} \cdot \sqrt{\frac{n+1}{2}} \tag{2.179}$$

The effectiveness factor as function of the generalized Thiele modulus is shown in Figure 2.26 for a slab and a sphere. Both curves coincide exactly for $\varphi_{\text{gen}} \to \infty$. The maximum deviations are in the order of 10–15%.

In general, the intrinsic kinetic parameters of a catalytic reaction under study are unknown. Therefore, the relationships based on the Thiele modulus cannot be used to estimate the influence of inner mass transfer on the measured overall reaction rate. Observed is the experimentally accessible efficient reaction rate, $r_{p,\,\text{eff}}$. In addition, the characteristic diffusion time in the porous pellet can be estimated. This allows to define a new modulus based on the characteristic effective reaction time $t_{r,\,\text{eff}}$ and the characteristic diffusion time in the particle, t_D. The ratio of these two values is known as *Weisz modulus*. We obtain for spherical pellets:

$$\psi_s^2 = \frac{t_D}{t_{r,\text{eff}}} = \frac{R_{\text{sphere}}^2}{D_e}\frac{c_s}{r_{p,\text{eff}}} = \eta_p \varphi_s^2 \tag{2.180}$$

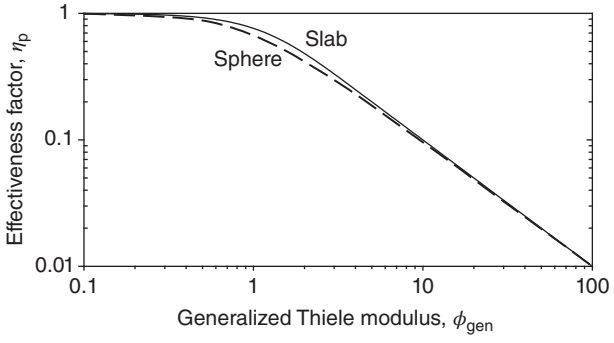

Figure 2.26 Effectiveness factor as function of the generalized Thiele modulus for different pellet geometries. (Adapted from Ref. [16], Figure 4.13 Copyright © 2012, Wiley-VCH GmbH & Co. KGaA.)

In analogy with the generalized Thiele modulus, we can define a Weisz modulus that applies to arbitrary pellet shapes and different reaction orders, n:

$$\psi_{\text{gen}}^2 = \frac{t_D}{t_{r,\text{eff}}} = \left(\frac{V_p}{A_p}\right)^2 \frac{n+1}{2} \frac{r_{p,\text{eff}}}{D_e c_s} = \eta_p \varphi_{\text{gen}}^2 \tag{2.181}$$

In Figure 2.27 a plot of the effectiveness factor against the generalized Weisz module for different reaction orders is shown. Using this relation, the effectiveness factor can be estimated based on the experimental kinetic results and the estimated diffusion coefficient.

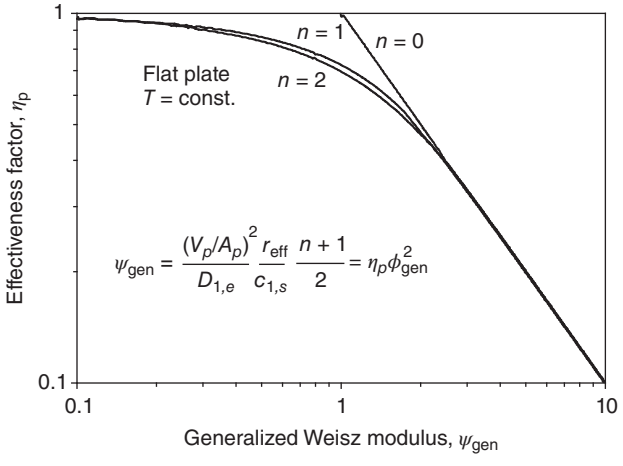

Figure 2.27 Effectiveness factor as function of the generalized Weisz modulus for different reaction orders. (Adapted from Ref. [16], Figure 4.14 Copyright © 2012, Wiley-VCH GmbH & Co. KGaA.)

Isothermal Yield and Selectivity The influence of transport phenomena on selectivity and yield is often more important than on the effective catalyst activity. The following analysis is restricted to two important schemes for complex reactions [28]:

parallel reactions: $A_3 \xleftarrow{k_2} A_1 \xrightarrow{k_1} A_2$ and
consecutive reactions: $A_1 \xrightarrow{k_1} A_2 \xrightarrow{k_2} A_3$.

We also neglect the effect of external mass transfer resistances and assume that the concentration at the pellet surface is identical to the bulk concentration ($c_{i,s} = c_{i,b}$).

In the case of *parallel reactions* the rate equations for the consumption of the reactant A_1 and concomitant formation of the desired product A_2 are given by:

$$\begin{aligned} -R_1 &= k_1 c_1^{n_1} + k_2 c_1^{n_2} \\ R_2 &= k_1 c_1^{n_1} \end{aligned} \tag{2.182}$$

with k_1 and k_2 as the intrinsic rate constants. The instantaneous or point selectivity is defined as the ratio of the A_2 production rate to the rate of reactant consumption:

$$s_{2,1} = \frac{R_2}{-R_1} = \frac{1}{1 + k_2/k_1 \cdot c_1^{(n_2 - n_1)}} = \frac{1}{1 + \kappa c_1^{(n_2 - n_1)}} \tag{2.183}$$

There is no influence of the concentration profile on selectivity in the case of equal order kinetics for the two reaction paths. If $n_1 \neq n_2$, the effective selectivity will be influenced by internal diffusion. As the influence of the internal concentration profile becomes more pronounced with increasing reaction order, the product selectivity will diminish, if the desired reaction has a higher order than the undesired. Otherwise, if the desired reaction has a lower kinetic order, the selectivity will be improved with increasing internal mass transfer resistance.

To discuss the influence of internal transport processes on *consecutive reactions*, we assume simple irreversible first order reactions. With k_1 and k_2 being the intrinsic rate constants, the production rate of A_2 and the disappearance of A_1 are given by:

$$\begin{aligned} R_2 &= k_1 c_1 - k_2 c_2 \\ -R_1 &= k_1 c_1 \end{aligned} \tag{2.184}$$

We obtain for the instantaneous selectivity in the kinetic regime:

$$s_{2,1} = \frac{R_2}{-R_1} = 1 - \frac{k_2}{k_1}\frac{c_{2,b}}{c_{1,b}} = 1 - \kappa \frac{c_{2,b}}{c_{1,b}}; \text{ with } \kappa = \frac{k_2}{k_1} \tag{2.185}$$

If transport resistances can be neglected, the concentration inside the catalyst pellet corresponds to the bulk concentration $c_i = c_{i,b}$. The instantaneous selectivity decreases with increasing conversion, X. In a catalytic fixed bed reactor with

plug flow behavior (see Section 2.3.4), the product yield can be determined by integration:

$$Y_{2,1} = \int_0^{X_L} s_{2,1} \mathrm{d}X$$
$$Y_{2,1} = \frac{1}{1-\kappa}[(1-X)^{\kappa} - (1-X)] \tag{2.186}$$

The yield increases up to a maximum and finally reaches zero for $X = 1$ as shown in Figure 2.28. The maximum depends on the ratio of the two rate constants and is given by

$$Y_{2,1,\max} = \kappa^{\kappa/(1-\kappa)} \text{ at } X_{\text{op}} = 1 - \kappa^{1/(1-\kappa)}; \text{ for } \kappa \neq 1 \tag{2.187}$$

To evaluate the influence of internal mass transfer on the product selectivity and yield, we have to solve the material balance for A_1 and A_2 in the porous catalyst. Assuming a flat plate and equal diffusion coefficient ($D_{1,e} = D_{2,e} = D_e$), we obtain with $c_{i,s} = c_{i,b}$:

$$\frac{\mathrm{d}^2 f_1}{\mathrm{d}Z^2} = \varphi_1^2 f_1; \qquad f_1 = \frac{c_1}{c_{1,s}} = \frac{c_1}{c_{1,b}};\ Z = \frac{z}{L};\ \varphi_1 = L\sqrt{\frac{k_1}{D_e}}$$
$$\frac{\mathrm{d}^2 f_2}{\mathrm{d}Z^2} = \varphi_2^2 \left(f_2 - \frac{1}{\kappa}\frac{c_{1,s}}{c_{2,s}} f_1 \right); \kappa = \frac{k_2}{k_1} \quad \varphi_2 = L\sqrt{\frac{k_2}{D_e}} \tag{2.188}$$

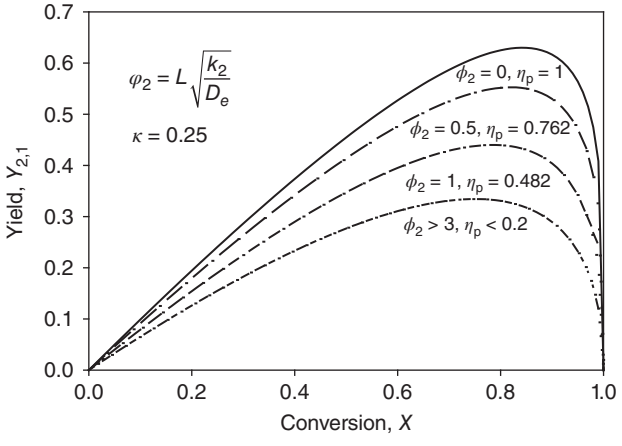

Figure 2.28 Effective product yield as function of conversion for consecutive reactions. Influence of internal mass transfer resistance. $\kappa = k_2/k_1 = 0.25$, initial product concentration $c_{2,0} = 0$. (Adapted from Ref. [16], Figure 4.15 Copyright © 2012, Wiley-VCH GmbH & Co. KGaA.)

With the concentration profile for the reactant A_1 given by Equation 2.171, the solution of the differential equation leads to:

$$f_1 = \frac{\cosh(\varphi_1 Z)}{\cosh(\varphi_1)}; \varphi_1 = L\sqrt{\frac{k_1}{D_e}}$$
$$f_2 = \left(1 + \frac{c_{1,s}}{c_{2,s}}\frac{1}{1-\kappa}\right)\frac{\cosh(\varphi_2 Z\kappa)}{\cosh(\varphi_2\kappa)} - \frac{c_{1,s}}{c_{2,s}}\frac{1}{1-\kappa}\frac{\cosh(\varphi_1 Z)}{\cosh(\varphi_1)}; \quad \varphi_2 = \sqrt{\kappa}\cdot\varphi_1 \tag{2.189}$$

The efficient instantaneous catalyst selectivity is given by the ratio of the efficient production rate of A_2 and the rate of reactant A_1 disappearance (see also Equation 2.172).

$$s_{2,1,\text{eff}} = \frac{R_{2,\text{eff}}}{-R_{1,\text{eff}}} = -\frac{(\mathrm{d}c_2/\mathrm{d}Z)_{Z=1}}{(\mathrm{d}c_1/\mathrm{d}Z)_{Z=1}} = \frac{1}{1-\kappa} - \left(\frac{c_{2,s}}{c_{1,s}} + \frac{1}{1-\kappa}\right)\cdot\sqrt{\kappa}\frac{\tanh(\varphi_2\sqrt{\kappa})}{\tanh(\varphi_2)} \tag{2.190}$$

For strong diffusion resistance within the catalyst pellet, Equation 2.190 can be simplified to:

$$s_{2,1,\text{eff}} = \frac{1}{1+\sqrt{\kappa}} - \sqrt{\kappa}\frac{c_{2,s}}{c_{1,s}} \text{ for } \varphi_2\sqrt{\kappa} > 3 \tag{2.191}$$

The overall product yield is obtained by integration of Equation 2.190 over a range of conversion. For a product concentration at the reactor inlet $c_{2,b,0} = 0$ the result is:

$$Y_{2,1,\text{eff}} = \frac{1}{1-\kappa}[(1-X)^{\Delta\varphi} - (1-X)]; \quad c_{2,b,0} = 0$$
$$\text{with } \Delta\varphi = \sqrt{\kappa}\frac{\tanh(\varphi_2)}{\tanh(\varphi_1)} = \sqrt{\kappa}\frac{\tanh(\varphi_2)}{\tanh(\varphi_2/\sqrt{\kappa})} \tag{2.192}$$

For very strong diffusional resistance Equation 2.192 can be simplified and the yield may be estimated from:

$$Y_{2,1,\text{eff}} = \frac{1}{1-\kappa}[(1-X)^{\sqrt{\kappa}} - (1-X)]; \quad c_{2,b,0} = 0 \tag{2.193}$$

The integral product yield as function of conversion for different values of the Thiele modulus is shown in Figure 2.28 for $\kappa = k_2/k_1 = 1/4$. It is obvious that internal diffusional resistance leads to a drastic decrease of the target product selectivity and yield. In the domain of practical interest with $\kappa < 1$, the maximum obtainable yield for strong diffusion resistance ($\varphi_2 \geq 3$, Equation 2.194) drops roughly to 50% of the value reached in the kinetic regime (Equation 2.187). At the same time the efficiency factor in the porous catalyst drops to $\eta_p < 0.2$ as indicated. This demonstrates the dramatic impact of pore diffusion limitation on the overall productivity of the catalytic process.

$$(Y_{2,1,\max})_{\varphi_2\geq 3} = \frac{\kappa^{[0.5\sqrt{\kappa}/(1-\sqrt{\kappa})]}}{1+\sqrt{\kappa}}; \text{ at } X_{\text{op}} = 1 - \kappa^{[0.5/(1-\sqrt{\kappa})]} \tag{2.194}$$

2.6.2.2 Nonisothermal Pellet

A large number of catalytic reactions are exothermic and are accompanied by thermal effects. For relatively fast intrinsic kinetics as compared to the mass and heat transfer phenomena, the development of internal temperature gradients can be expected. Heat and mass transfer balances have to be solved simultaneously to estimate concentration and temperature profiles under steady-state conditions. As the reaction rate depends exponentially on temperature, the resulting temperature and concentration profiles have to be calculated by numerical methods.

$$D_e \frac{d^2 c_1}{dz^2} - (-R_1) = 0$$
$$\lambda_e \frac{d^2 T}{dz^2} - (-R_1)(-\Delta H_r) = 0 \tag{2.195}$$

where $(-\Delta H_r)$ is the reaction enthalpy and λ_e is the effective thermal conductivity in the porous pellet. As the reaction rate is the same in both balances, we obtain:

$$\frac{D_e(-\Delta H_r)}{\lambda_e} \frac{d^2 c_1}{dz^2} = \frac{d^2 T}{dz^2} \tag{2.196}$$

With the surface concentration and temperatures $c_{1,s}$ and T_s, we obtain after integration a linear relationship between internal temperature and reactant concentration:

$$T - T_s = (-\Delta H_r)\frac{D_e}{\lambda_e}(c_{1,s} - c_1) \tag{2.197}$$

The largest possible temperature difference in the particle is attained, when the concentration in the particle center becomes $c_{1,\text{center}} = >0$.

$$(T_{\text{center}} - T_s)_{\max} = (-\Delta H_r)c_{1,s}\frac{D_e}{\lambda_e} \tag{2.198}$$

Obviously, the maximum temperature difference will depend on the reaction enthalpy and the ratio between effective diffusion and effective thermal conductivity.

If we refer the maximum temperature difference to the surface temperature, we get the dimensionless so-called Prater number, β.

$$\beta = \frac{\Delta T_{\max}}{T_s} = \frac{(-\Delta H_r)c_{1,s}}{T_s}\frac{D_e}{\lambda_e} \tag{2.199}$$

For exothermic reactions the temperature inside the pellet will be higher than the surface temperature. Because of the exponential increase of the reaction rate, the temperature effect can overcompensate the lower concentration in the pellet. An example is shown in Figure 2.29 where the effectiveness factor is plotted versus the Thiele modulus for an Arrhenius number of $\gamma = 20$ and different Prater numbers.

The curves shown were obtained by numerical integration by Weisz and Hicks [30]. Efficiency factors higher than one can be expected at relatively low Thiele modulus and high Prater and Arrhenius numbers. At large values of φ, the

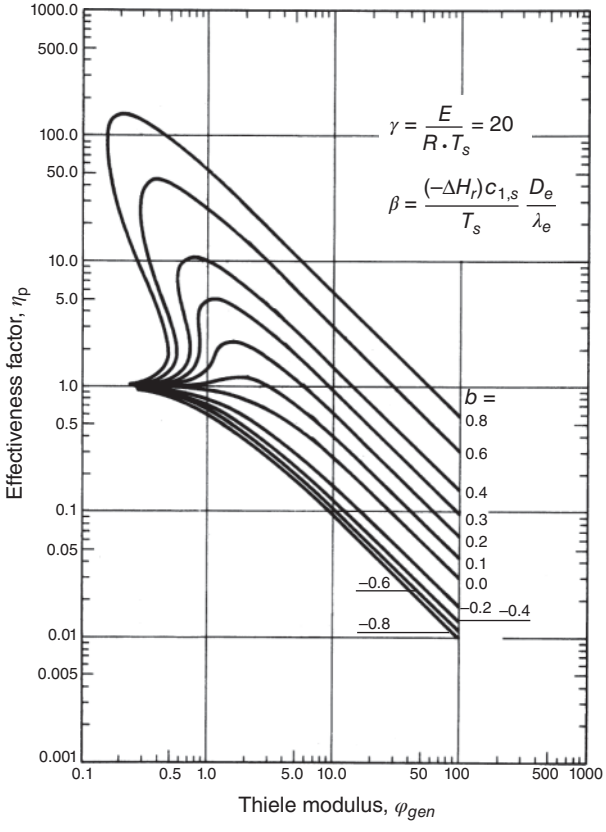

Figure 2.29 Effectiveness factor as function of the Thiele modulus. Nonisothermal sphere, first order reaction [30]. (Adapted with permission from Elsevier.)

effectiveness factor becomes inversely proportional to the Thiele modulus, as observed at isothermal conditions. Besides the increase of the observed reaction rate because of the high internal temperature, multiple steady states are predicted for reactions with high Arrhenius numbers and high Prater numbers. In the region of multiple steady states, different temperature and concentration profiles for the same Thiele modulus may exist leading to different effectiveness factors. This behavior is shown in Figure 2.29 for $0.2 < \varphi < 1$ and $\beta > 0.2$.

For majority of industrial catalysts the effective heat conductivity is in the order of $0.2 < \lambda_e < 0.5$ and efficient diffusion coefficients for gas phase reactions are in the order of 10^{-5} to 10^{-6} m^2 s^{-1}. Therefore, Prater numbers seldom exceed values of $\beta = 0.1$ and the maximum temperature in the pellet center is seldom higher than $\Delta T_{max} = 10$ K.

In summary, temperature differences between gaseous bulk and catalyst surface are much more important as discussed in Section 2.6.1.2.

2.6.2.3 Combination of External and Internal Transfer Resistances

In the previous chapters we discussed the influence of internal mass and heat transfer by neglecting external transport phenomena. Hence, we assumed that concentrations and temperature at the outer surface of the catalyst particle and the bulk of the fluid are the same. But this assumption is not justified under certain conditions and concentration and temperature profiles inside and outside the porous catalyst must be considered.

2.6.2.4 Internal and External Mass Transport in Isothermal Pellets

If the efficient reaction rate is high enough, the reactant concentration drops significantly across the external boundary layer as indicated in Figure 2.18. In this case the surface concentration is lower compared to the bulk of the fluid phase ($c_{1,s} < c_{1,b}$). First we will neglect eventual heat effects and assume equal temperatures in the fluid and the catalyst particle ($T = T_s = T_b$). To determine the concentration profile in the particle, we first have to calculate the concentration at the external surface. This will be done based on the mass balance for the reactant A_1. At steady state, the molar flux of A_1 from the bulk to the external surface must be equal to the effective rate of transformation (see Equation 2.137).

$$J_1 = k_m(c_{1,b} - c_{1,s}) = \frac{-R_{1,p,\text{eff}}}{a_p} \tag{2.200}$$

For a simple irreversible first order reaction we obtain:

$$k_m(c_{1,b} - c_{1,s}) = \frac{\eta_p k_r c_{1,s}}{a_p} \text{ with } \eta_p \text{ the internal effectiveness factor} \tag{2.201}$$

Solving Equation 2.201 for the unknown surface concentration:

$$c_{1,s} = \frac{c_{1,b}}{1 + \eta_p k_r/(k_m a_p)} \tag{2.202}$$

If we introduce the ratio between the characteristic diffusion time in the pellet t_D and the external mass transfer time t_m we will get a clear physical interpretation of this relationship. The mentioned ratio is known as the *mass Biot number*, Bi_m.

$$Bi_m = \frac{t_D}{t_m} = \frac{L_c^2}{D_e} k_m a_p \text{ with } L_c \text{ the characteristic length of the pellet} \tag{2.203}$$

Introducing the Biot number in Equation 2.202 yields:

$$c_{1,s} = \frac{c_{1,b}}{1 + \eta_p \frac{k_r L_c^2}{D_e} \cdot \frac{1}{Bi_m}} = \frac{c_{1,b}}{1 + \eta_p \frac{\varphi^2}{Bi_m}} \tag{2.204}$$

The overall effectiveness factor is defined as the ratio between the effective transformation rate and the rate at constant bulk concentration.

$$\eta_{ov} = \frac{-R_{1,\text{eff}}}{-R_{1,b}} = \frac{-R_{1,\text{eff}}}{k_r c_{1,b}} = \frac{\eta_p c_{1,s}}{c_{1,b}} \tag{2.205}$$

In combination with Equation 2.204 we obtain:

$$\eta_{ov} = \frac{\eta_p}{1 + \eta_p \frac{\varphi^2}{Bi_m}} = \frac{1}{\frac{1}{\eta_p} + \frac{\varphi^2}{Bi_m}} \tag{2.206}$$

For a catalyst in the form of a flat plate the effectiveness factor is given by $\eta_p = \tanh \varphi_L / \varphi_L$ (Equation 2.174) and the overall effectiveness factor can be expressed as a function of the Thiele modulus and the Biot number.

$$\eta_{ov} = \frac{\tanh \varphi}{\varphi \left(1 + \frac{\varphi \cdot \tanh \varphi}{Bi_m}\right)} \tag{2.207}$$

The relationship shown in Equation 2.207 suffers from the fact that the Thiele modulus must be specified to estimate the catalyst efficiency. This is, in general, not possible as the intrinsic kinetics is not known. It is, therefore, more convenient to relate the overall effectiveness factor to the Weisz modulus, which is based only on observable parameters.

The catalyst efficiency decreases strongly at small mass Biot numbers as seen in Figure 2.30. This is because of the reduced reactant concentration on the external pellet surface. In contrast, external mass transfer influences can be neglected at $Bi_m > 100$. In practice, catalytic particles are in the range of several millimeters and the mass Biot numbers are in the order of 100–200. Hence, the overall effectiveness factor is almost entirely determined by the intraparticle diffusion.

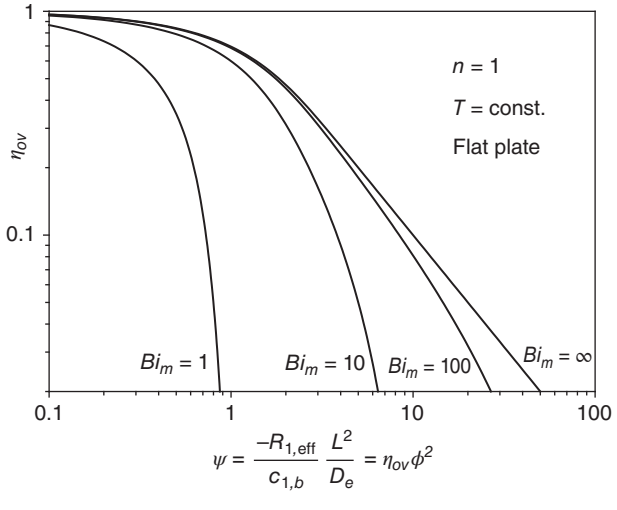

Figure 2.30 Overall effectiveness factor as a function of the Weisz modulus for different mass Biot numbers (isothermal, irreversible first order reaction in a porous slab). (Adapted from Ref. [16], Figure 4.17 Copyright © 2012, Wiley-VCH GmbH & Co. KGaA.)

2.6.2.5 The Temperature Dependence of the Effective Reaction Rate

As pointed out, the influence of mass transfer on the observed reaction rate depends on the ratio between the characteristic reaction time and the characteristic time for mass transfer. By increasing the temperature, the intrinsic reaction rate increases more strongly (exponentially) than the rates of external and internal mass transfer. Consequently, the Thiele modulus and the second Damköhler number augment with increasing temperature, and transport phenomena become more and more important and will finally control the transformation process. In addition, the temperature dependence of the observed reaction rate will change as indicated.

At low temperatures the process is controlled by the intrinsic chemical kinetics and the rate constant increases exponentially following Arrhenius law:

$$k = k_0 \exp\left(\frac{-E}{RT}\right) \tag{2.208}$$

with k_0 the frequency factor and E the intrinsic activation energy.

The temperature dependence of the diffusion process is represented by proportionality to $T^{3/2}$ but can be also approximated by an Arrhenius equation:

$$D_e = D_{e,0} \exp\left(\frac{-E_D}{RT}\right); \text{ with } 5 < E_D < 10\,\text{kJ mol}^{-1} \tag{2.209}$$

This is not a theoretical dependence of D_e on temperature but is useful for the following discussions. At strong influence of internal diffusion on the reaction rate, the effectiveness factor was found to be inversely proportional to the Thiele modulus (e.g., Equation 2.176). Accordingly, the effective rate constant is given by:

$$k_{\text{eff}} = \frac{k}{L\sqrt{k/D_e}} = \frac{1}{L}\sqrt{k \cdot D_e} \tag{2.210}$$

For the temperature dependence follows:

$$k_{\text{eff}} = \frac{\sqrt{k_0 D_{e,0}}}{L} \exp\left(-\frac{E + E_D}{2 \cdot RT}\right) \tag{2.211}$$

Normally $E \gg E_D$, as diffusion is not very temperature sensitive, so the observed apparent activation energy is about one-half of the true value when pronounced internal concentration profiles are present (Figure 2.31).

Further temperature increase will diminish the reactant concentration on the outer pellet surface as the influence of external mass transfer becomes important. Finally, interphase mass transfer will be the rate controlling step and the surface concentration drops to zero. Under those conditions, the apparent activation energy corresponds to E_{D}.

Besides the apparent activation energy, the effective reaction order changes during the transition from the kinetic to the diffusion controlled regime. A first order reaction will be observed under external mass transfer control. The effective reaction order observed approaches $n_{\text{app}} = (n + 1)/2$ for severe influence of intraparticle diffusion.

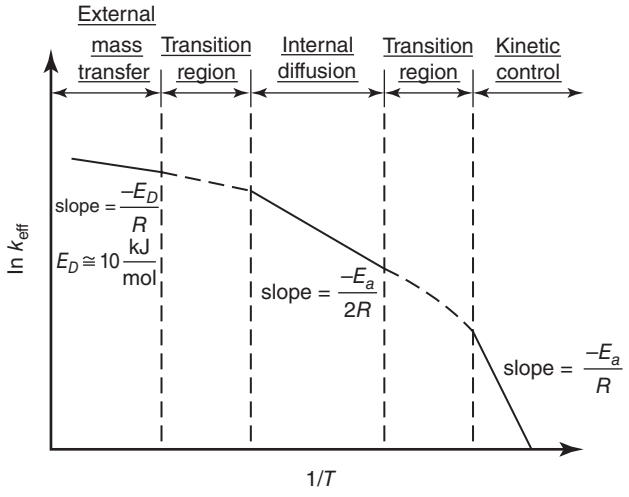

Figure 2.31 Arrhenius plot for heterogenous catalytic reactions. Transition from the kinetic regime to mass transfer controlled regime.

2.6.2.6 External and Internal Temperature Gradient

In the case of fast highly exothermic or endothermic reactions, temperature gradients inside the porous catalyst and temperature differences between the fluid phase and catalyst surface cannot be neglected. Depending on the physical properties of the fluid and the solid catalyst, important temperature gradients may occur. The relative importance of internal to external temperature profiles can be estimated based on the relationships presented in Sections 2.6.1.2 and 2.6.2.2. According to Equation 2.158 the temperature difference between bulk and outer pellet surface is:

$$T_s - T_b = \frac{(-\Delta H_r)}{h \cdot a_p} \cdot r_{\text{eff}} \quad \text{with } r_{\text{eff}} = k_m a_p (c_{1,b} - c_{1,s})$$

$$T_s - T_b = (-\Delta H_r)\frac{k_m}{h}(c_{1,b} - c_{1,s}) \tag{2.212}$$

With the Chilton-Colburn analogy we can replace the ratio k_m/h and obtain (see Equation 2.161)

$$T_s - T_b = (-\Delta H_r)\frac{1}{\rho c_p}\left(\frac{\text{Pr}}{Sc}\right)^{2/3}(c_{1,b} - c_{1,s}) \tag{2.213}$$

For large internal diffusional resistance, the concentration of the reactant in the pellet center drops to zero. In this situation the temperature difference between the outer surface and the center of a porous catalyst pellet is maximal and given by Equation 2.198.

In Equation 2.214 the temperature difference between bulk and pellet surface is compared with the maximum internal temperature gradient. The ratio between

Table 2.1 Physical properties of fluid/solid systems [13].

	Gas	Liquid	Porous solid
D or D_e ($m^2 \cdot s^{-1}$)	$10^{-5}-10^{-4}$	$10^{-10}-10^{-9}$	$10^{-7}-10^{-5}$
λ or λ_e ($W \cdot m^{-1}\ K^{-1}$)	$10^{-3}-10^{-1}$	$10^{-2}-10$	$10^{-2}-1$
$\rho\ c_p$ ($J \cdot m^{-3}\ K^{-1}$)	$10^{2}-10^{5}$	$10^{5}-10^{7}$	$10^{6}-10^{7}$

these two temperature differences depends on the ratio of the mass Biot to the thermal Biot numbers.

$$\frac{T_s - T_b}{(T_{\text{center}} - T_s)_{\max}} = \frac{k_m}{h}\frac{\lambda_e}{D_e}\frac{c_{1,b} - c_{1,s}}{c_{1,s}} = \frac{Bi_m}{Bi_{\text{th}}}\frac{c_{1,b} - c_{1,s}}{c_{1,s}}$$
$$\text{with } Bi_{\text{th}} = \frac{h \cdot L}{\lambda_e};\ Bi_m = \frac{k_m \cdot L}{D_e} \tag{2.214}$$

In Table 2.1 the order of magnitude of some physical properties of fluid/solid systems are summarized. On the basis of these values we can conclude that for gas/solid systems the ratio of Bi_m/Bi_{th} is in the range of $10-10^4$. Hence, the temperature gradient in the external boundary layer is much more important than within the pellet under usual reaction conditions:

$$(T_s - T_b) >> (T_{\text{center}} - T_s);\ \text{gas/solid system} \tag{2.215}$$

In contrast, we expect a higher temperature difference within the pellet in liquid/solid systems.

2.6.3 Criteria for the Estimation of Transport Effects

For the catalyst development and optimization as well as for the correct reactor design, it is important to ascertain the influences of transport phenomena on the reaction kinetics. It is essential that criteria for estimating transport effects are based on what is measurable or observable [31, 32].

One way to estimate the influence of transport processes is to use directly experimental results observed under given experimental conditions. In general, the experimentalist has information concerning observed reaction rates, bulk reactant concentrations, and temperature, as well as the catalyst pellet form and dimensions. With these details at hand, the Weisz module can be estimated. For example, for spherical catalytic particles, see Equation 2.180.

Each of the ψ_s values is experimentally accessible and the effectiveness factor can be computed such as shown in Figure 2.32. Hence, a set of graphs can be prepared relating ψ_s to η with the Arrhenius and Prater numbers as parameters and allowing estimation of the effectiveness factors directly from experimental results. An important number of criteria for estimating the influence of transport

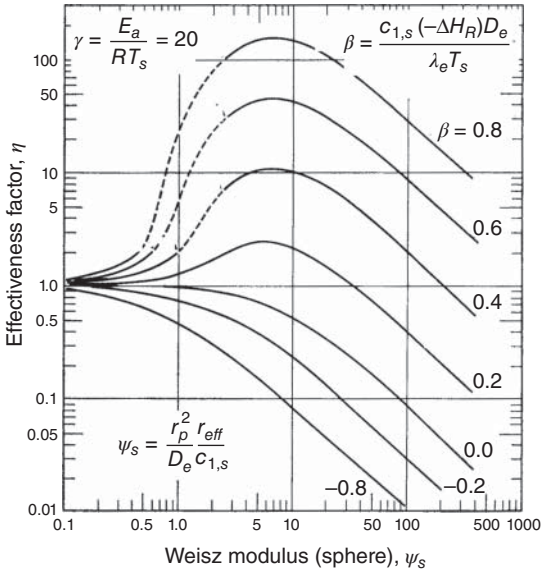

Figure 2.32 Effectiveness factor in terms of the experimentally observable Weisz modulus. First order reaction, sphere [30]. (Adapted with permission from Elsevier.)

phenomena on catalytic reaction rates are published in the open literature. In general, these criteria are derived assuming that transport effects do not alter the true rate by more than ±5%. Because of the uncertainty involved in estimating the different parameters, the application of the criteria should be done in a conservative manner. The observed values should be at least several times or even an order of magnitude better than those proposed.

The most general of the criteria (Equation 6 in Table 2.2) ensures the absence of any internal and external concentration and temperature gradient. But a problem may arise because of compensation between mass and heat transport. This situation will occur if $\gamma \cdot \beta \cong n$. Therefore, it may be better to respect separately the criteria for isothermicity.

It is disturbing that criteria for the absence of heat effects are based on the true activation energy, which is not observable, if mass transfer affects the rate of reaction. A critical discussion of the experimental results and a prudent application of the criteria are, therefore, indispensable.

2.7 Summary

In this chapter, the fundamentals of chemical reaction engineering are presented. The basic definitions along with the material balance of different types of ideal reactors and their design equations are discussed.

Table 2.2 Experimental criteria for the absence of inter and intra transport phenomena ($0.95 < \eta < 1.05$) for simple irreversible reactions.

1	Absence of interphase concentration gradients in isothermal systems	$\frac{r_{p,\text{eff}} d_p}{2k_m c_{i,b}} < \frac{0.15}{\lvert n \rvert}$
2	Absence of interphase temperature gradients. The criterion is independent whether intraparticle gradients exist or not	$\frac{(-\Delta H_r) r_{p,\text{eff}} d_p}{2h \cdot T_b} \frac{E}{RT_b} < 0.15$
3	Absence of intraparticle/interphase gradients	$\frac{r_{p,\text{eff}} d_p^2}{4c_{i,b} D_e} < \frac{1+\gamma \cdot \chi}{\lvert n-\gamma \cdot \beta \rvert (1+0.33\,\text{n} \cdot \text{w})}$ $\chi = \frac{(-\Delta H_r) r_{p,\text{eff}} d_p}{2h \cdot T_b}, w = \frac{r_{p,\text{eff}} d_p}{2c_{i,b} k_m}$
4	Absence of concentration profiles within an isothermal porous catalyst pellet	$< 6 \;\; n = 0$ $\frac{r_{p,\text{eff}} d_p^2}{4D_e c_{i,s}} < 0.6 \;\; n = 1$ $< 0.2 \;\; n = 2$
5	Absence of intraparticle temperature profile	$\frac{(-\Delta H_r) r_{p,\text{eff}} d_p^2}{4\lambda_e T_s} < \frac{RT_s}{E}$
6	Absence of combined effect of temperature and concentration gradients	$\frac{r_{p,\text{eff}} d_p^2}{4\, c_{1,b} D_e} < \frac{1}{\lvert n-\gamma \cdot \beta \rvert}; \gamma = \frac{E}{RT_b}, \beta = \frac{(-\Delta H_r D_e c_{1,b})}{\lambda T_b}$

Adapted from Ref. [13].

The homogenous reactions are defined as the reactions taking place in gas or liquid phase. The rates of the homogenous reactions are usually determined experimentally and their dependence on the reactant concentration is represented by a power rate law. In general, it is assumed that the temperature dependence of the rate constant for most homogenous reactions obeys Arrhenius equation. Catalytic reactions are discussed based on different types of catalysts used: a substance dissolved in reaction mixture (homogenous catalysis), an enzyme (enzymatic catalysis), or a solid substance (heterogenous catalysis). In homogenous and enzymatic catalysis, it is assumed that a complex is formed between the reactant and a dissolved catalyst and the product is then formed from this complex. This simplified kinetic scheme allows to obtain a generalized rate equation also known as *Michaelis–Menten equation*. In heterogenously catalyzed reactions, it is important to identify the rate-determining step in order to obtain a rate equation. Generally, the surface reaction between adsorbed reactants is considered as the rate-limiting step.

The kinetics of the many commercially important reactions is derived from experimental investigations that are further simplified with substantive assumption on reaction mechanism. During the kinetics study of heterogenous catalytic reactions, mass and heat transfer may affect the observed kinetics and must be avoided.

2.8 List of Symbols

a	Activity factor	—
A_p	Pallet outer surface	m^2
a_p	Specific external surface area of the pellet	$m^2\ m^{-3}$
c_b, c_{cat}, c_i^*, c_s	Bulk concentration, concentration of catalyst, concentration of species A_i at equilibrium, concentration at surface	$mol\ m^{-3}$
c_{dea}	Concentration of deactivating component which cause deactivation	$mol\ m^{-3}$
$\overline{C}_w$	Total heat capacity of the reactor	$J\ K^{-1}$
E_d, E_D	Activation energy of deactivation, of diffusion	$J\ mol^{-1}$
E_{sys}	Energy of system	J
$\dot{E}_{in}$, $\dot{E}_{out}$	Rate of energy in, rate of energy out	$J\ s^{-1}$
$\hat{H}$	Molar enthalpy	$J\ mol^{-1}$
I_0, I_1	Bassel functions of zero and first order	—
k_i	Adsorption rate constant	variable
k_{-i}	Inverse adsorption rate constant	variable
k_d	Deactivation constant	varibale
K_M	Michaelis constant	$mol\ m^{-3}$
L_c	Characteristic length of pallet	m
m	Mass	kg
r_{ads}, r_{des}	Rates of adsorption, rates of desorption	$mol\ m^{-2}\ s^{-1}$
r_d	Rate of deactivation	—
r_p	Rate of reaction per unit volume of catalyst pallet	$mol\ m^{-3}\ s^{-1}$
S	Entropy	$J\ K^{-1}$
t'	Operating time (or lifetime) of the catalyst	s
t_a, t_R, t_{cycle}	Shut-down time, reaction time, batch cycle time	s
$\hat{U}_i$	Molar energy	$J\ mol^{-1}$
V_{film}	Film volume	m^3
$\hat{V}_i$	Molar volume of species A_i	$m^3\ mol^{-1}$
$X^{\#}$	Catalyst substrate complex	—
y	Mole fraction	—
Z_{tot}	Total concentration of active sites	—
α	Expansion factor	—
δ_i	Interfacial film thickness in phase i	m
ΔH_a	Heat of adsorption	$J\ mol^{-1}$
θ_i, θ_v	Fractional surface coverage by species A_i, fraction of vacant sites	—
κ	Ratio of reaction rates	—
η_{ov}, η_{ex}, η_p	Overall effectiveness factor, external, of porous catalyst	—
τ_p	Tortuosity	—
φ	Thiele modulus	—
ψ_s, ψ_{gen}	Weisz modulus, generalWeisz modulus	—

References

1. McGlashan, M.L. (1970) Manual of symbols and terminology for physicochemical quantities and units. *Pure Appl. Chem.*, **21**, 1–44.
2. Wedler, G. (1982) *Lehrbuch der Physikalischen Chemie*, Verlag Chemie, Weinheim.
3. Roulet, R. (2004) *Elements Fondamentaux de Chimie* (ed. EPFL), Ecole Polytechnique Fédérale de Lausanne.
4. Taube, R. (1988) *Homogene Katalyse*, Akademie-Verlag, Berlin.
5. Dalko, P.I. and Moisan, L. (2004) In the golden age of organocatalysis. *Angew. Chem. Int. Ed.*, **43** (39), 5138–5175.
6. Broenstedt, J.N. (1923) Einige Bemerkungen über den Begriff der Säuren und Basen. *Recl. Trav. Chim. Pays-Bas*, **42** (8), 718–728.
7. Lowry, T.M. (1923) The uniqueness of hydrogen. *J. Soc. Chem. Ind.*, **42** (3), 43–47.
8. Flaschel, E. (1992) Enzyme kinetics and reactor design, in *Biocatalytic Production of Amino Acids and Derivates* (eds D. Rozzel and F. Wagner), Hanser Verlag, München.
9. Flaschel, E., Raetz, E., and Renken, A. (1982) The kinetics of lactose hydrolysis for the β-galactosidase from Aspergillus niger. *Biotechnol. Bioeng.*, **24**, 2499–2518.
10. Raetz, E. (1982) *Développement d'un réacteur à membrane pour la catalyse enzymatique*, Ecole Polytechnique Fédérale de Lausanne.
11. Beckberger and Watson, K.M. (1948) Catalytic dehydrogenation of normal butenes to butadiene in the presence of steam. *Chem. Eng. Progress*, **6**, (3), 229–248.
12. Cornils, B., Herrmann, W.A., Horváth, I.T., Leitner, W., Mecklenburg, S., Olivier-Bourbigou, H., and Vogt, D. (eds) (2005) *Multiphase Homogeneous Catalysis*, vol. 1, Wiley-VCH Verlag GmbH, Weinheim.
13. Baerns, M., Hofmann, H., and Renken, A. (2002) *Chemische Reaktionstechnik*, 3rd edn, Wiley-VCH Verlag GmbH, Weinheim.
14. Levenspiel, O. (1999) *Chemical Reaction Engineering*, 3rd edn, John Wiley & Sons, Inc., New York, etc.
15. Trambouze, P. and Euzen, J.-P. (2002) *Les réacteurs chimiques*, TECHNIP, Paris.
16. Renken, A. and Kiwi-Minsker, L. (2012) in *Catalytic Engineering Principles. Catalysis: From Molecular to Reactor Design* (eds M. Beller, A. Renken, and R.A.v. Santen), Wiley-VCH Verlag GmbH, Weinheim, pp. 67–110.
17. Mehnert, C.P., Cook, R.A., Dispenziere, N.C., and Afeworki, M. (2002) Supported ionic liquid catalysis – a new concept for homogeneous hydroformylation catalysis. *J. Am. Chem. Soc.*, **124** (44), 12932–12933.
18. Mehnert, C.P., Mozeleski, E.J., and Cook, R.A. (2002) Supported ionic liquid catalysis investigated for hydrogenation reactions. *Chem. Commun.*, **8** (24), 3010–3011.
19. Riisager, A., Eriksen, K.M., Wasserscheid, P., and Fehrmann, R. (2003) Propene and 1-octene hydroformylation with silica-supported, ionic liquid-phase (SILP) Rh-phosphine catalysts in continuous fixed-bed mode. *Catal. Lett.*, **90** (3–4), 149–153.
20. Riisager, A., Wasserscheid, P., Van Hal, R., and Fehrmann, R. (2003) Continuous fixed-bed gas-phase hydroformylation using supported ionic liquid-phase (SILP) Rh catalysts. *J. Catal.*, **219** (2), 452–455.
21. Riisager, A., Fehrmann, R., Haumann, M., and Wasserscheid, P. (2006) Supported Ionic Liquid Phase (SILP) catalysis: an innovative concept for homogeneous catalysis in continuous fixed-bed reactors. *Eur. J. Inorg. Chem.*, **4**, 695–706.
22. Renken, A. (2010) Chemical reaction engineering aspects for heterogenized molecular catalysis, in *Heterogenized Homogeneous Catalysts for Fine Chemical Production. Materials and*

Processes (eds P. Barbaro and F. Liguori), Springer.
23. Kashid, M.N., Renken, A., and Kiwi-Minsker, L. (2011) Microstructured reactors and supports for ionic liquids. *Chem. Eng. Sci.*, **66** (7), 1480–1489.
24. Boudart, M. and Djega-Mariadassou, G. (1982) *La cinétique des réactions en catalysehétérogène*, Masson, Paris etc.
25. Froment, G.F. and Bischoff, K.B. (1979) *Chemical Reactor Analysis and Design*, John Wiley & Sons, Inc., New York.
26. Butt, J.B. and Petersen, E.E. (1988) *Activation, Deactivation and Poisoning of Catalysts*, Academic Press, San Diego, CA.
27. Cassiere, G. and Carberry, J.J. (1973) Interphase catalytic effectiveness factor: activity, yield and non-isothermality. *Chem. Eng. Educ.*, **7** (1), 22–26.
28. Dittmeyer, R. and Emig, G. (2008) in *Handbook of Heterogeneous Catalysis* (eds G. Ertl, H. Knözinger, F. Schüth, and J. Weitkamp), Wiley-VCH Verlag GmbH, Weinheim, pp. 1727–1784.
29. Aris, R. (1957) On the shape factors of irregular particles-I, *Chem. Eng. Sci.*, **6** (6), 262–268.
30. Weisz, P.B. and Hicks, J.S. (1962) The behaviour of porous catalyst particles in view of internal mass and heat diffusion effects. *Chem. Eng. Sci.*, **17** (4), 265–275.
31. Mears, D.E. (1971) Tests for transport limitations in experimental catalytic reactors. *Ind. Eng. Chem. Process Des. Dev.*, **10** (4), 541–547.
32. Mears, D.E. (1971) Diagnostic criteria for heat transport limitations in fixed bed reactors. *J. Catal.*, **20** (2), 127–131.